

Chapter 4.1.1 of Climate System Modeling

Tropical Pacific ENSO models: ENSO as a mode of the coupled system

Mark A. Cane

December 3, 2004

The most dramatic, most energetic, and best defined pattern of interannual variability is the global set of climatic anomalies referred to as ENSO, an acronym derived from its oceanographic component, El Niño, and its atmospheric component, the Southern Oscillation. Occurring irregularly, but about every 4 years on average, ENSO warm events directly effect the climate of more than half the planet, often exacting a heavy toll in human life and economic well-being.

The devastating consequences of the 1982/83 ENSO warm event, the most extreme in at least a century, are graphically illustrated in Canby (1984). In Australia the worst drought ever recorded spawned firestorms that incinerated whole towns. The same drought conditions resulted in the burning of millions of acres of rainforest in Borneo. There were also severe droughts in the Nordeste region of Brazil, in the Sahel, and in Southern Africa. Normally arid regions of Peru and Ecuador were inundated by more than 3m of rain, causing great loss of life and destruction of the transportation infrastructure. Drastic changes in the tropical Pacific Ocean resulted in mass mortality of fish and bird life. All in all, \$8 billion in damages and the loss of 2000 lives have been attributed to the 1982/83 ENSO event.

While the consequences of the warm events has long been appreciated (some historical remarks are given below), awareness of the importance of the cold extremes of the ENSO cycle has developed quite recently. The linking of the cold event of 1988 to the drought in North America (Trenberth et al, 1988), was but one of the global consequences (cf Ropelewski and Halpert, 1987).

ENSO has a number of special relations to the issue of greenhouse warming motivating so much of the current interest in the climate system (including this book). The ultimate realization of all climate fluctuations, even those, like the march of the seasons – or greenhouse warmin– which are externally forced, depends on complex internal feedbacks within the climate system. ENSO is the prime example of variability stemming entirely from the internal workings of the climate system. Generated by the interaction of ocean and atmosphere, it embodies physics essential to longer term climate variability.

The ongoing controversy about detection of the greenhouse signal in the climate record turns in part on whether a secular increase in global temperature can be said to have emerged from the noise. In this case “noise” means the natural (and thus “normal”) variability of the earth’s climate system. Any statistical test intended to decide this question must rely on some model

for this noise. ENSO accounts for a significant fraction of natural variability, with a warm event increasing the global temperature by as much as several tenths of a degree {Ed :i expect there a temperature time series fig elsewhere in the book to reference? If not, perhaps one should go here.} Thus a model which accounts explicitly for ENSO reduces the background noise, allowing the secular change to stand out more decisively (eg Jones, 1988). The warming then appears as more statistically significant, though such a test still cannot establish its cause.

Some have drawn support for the greenhouse warming scenario from the widely accepted fact that the decade of the 1980s is the warmest in the instrumental record. Others dispute this interpretation, often by pointing out that this status rests on the two ENSO events in the decade, the extreme event of 1982-83 and the long-lived event of 1986-87. The two may not be inconsistent explanations, for we cannot now rule out the possibility that the strength of the ENSO events in the 1980s was a manifestation of greenhouse warming. Fig. 1, which will be discussed at some length below, illustrates this possibility. An ENSO model run with present climate conditions as a background state is compared with a run based on a greenhouse warming scenario. Events in the latter are more frequent and larger in amplitude. The question of the effects of increased greenhouse gases on interannual variability is of obvious importance. Societies are far better at coping with predictable and regular changes than with irregular departures from normal conditions. For many areas of the globe an increase in the severity or frequency of ENSO events would be devastating. Moreover, the possibility of alterations in the characteristics of climate variability complicates the research task of identifying the “fingerprint” of greenhouse warming.

The ENSO modeling experience also can provide valuable lessons for more comprehensive climate system modeling efforts. It is arguably the most advanced example of modeling two-way interactions between the atmosphere and ocean. It is one of the few examples of successful prediction of climate variations by objective means, and the only verified example where the prediction has been carried out with a dynamical model, now the common method in weather prediction.

ENSO modeling began from a base of useful hypotheses as to the mechanisms governing ENSO, hypotheses developed from a brilliant analysis of data too meager to be conclusive. This background and our subsequent picture of the workings of ENSO are reviewed in the next section. A variety of models followed (see Sec 3), including relatively simple models providing important analytical tools, and also “intermediate” models, which, while less complex than the comprehensive GCMs, achieved recognizable simulations of ENSO. Their results validated some of the earlier ideas and allowed further theoretical advances. They also demonstrated some predictive skill (Sec 4), which is both valuable in its own right and also increases confidence in their general correctness. Sec 5 considers efforts along the more difficult path of coupling GCMs. A final section discusses implications of the ENSO modeling experience.

This chapter is organized with some attention to the history of ENSO research in the belief that this best reveals its lessons for this next stage in climate modeling. The ENSO literature is vast and the account here is necessarily sketchy. Good brief reviews, though already somewhat dated are Rasmusson (1985) and Cane (1986). A thorough treatment with emphasis on the physics of ENSO is the recent monograph by Philander (1990). The collection edited by Glantz et al (1990) provides a more succinct account of relevant physics amid its emphasis on the global impacts of ENSO.

2. Our understanding of the mechanisms of ENSO

El Niño historically refers to a massive warming of the coastal waters off Peru and Ecuador. It is accompanied by torrential rainfall, often resulting in catastrophic flooding. Widespread mortality of fish and guano birds further damages the local economy. El Niño events have been documented back to 1726 (Quinn et al,1978) and there is other evidence indicating occurrences for at least a millenium prior to that (Quinn:etal1987).

The atmospheric component of ENSO, the Southern Oscillation, is a more recent discovery. Although the term is sometimes used to refer to the global complex of climatic variations, the SO is specifically an oscillation in surface pressure (and thus atmospheric mass) between the southeastern Pacific and Australian-Indonesian regions. A convenient Southern Oscillation index (SOI) is the pressure difference between Tahiti and Darwin. The seminal figure in delineating the SO and showing its worldwide associations was Sir Gilbert Walker, Director-General of the Observatory in India. Walker assumed his post in 1904, shortly after the famine resulting from the monsoon failure in 1899 (an El Niño year); his goal was to predict the monsoon fluctuations, an activity begun by his predecessors after the disastrous monsoon of 1877 (also an El Niño year).

Walker was already aware of work dating from just before the turn of the century which described the sea-level pressure swing between South America and India-Australia. Over the next 3 decades he added correlates from all over the globe to this primary SO signal: rainfall in India and in the central equatorial Pacific; temperatures in southeastern Africa, southwestern Canada, the southeastern United States; etc. This work, being purely empirical and based on records too short to establish its reliability, was long regarded with considerable skepticism. However, in recent years Walker's correlations have been found to hold up when examined with more than 50 years of new data (see especially Horel and Wallace, 1981, and Ropelewski and Halpert, 1987).

Oddly, Walker missed the connection to El Niño. It only became widely appreciated after the revival of interest in the SO in the 1960s, principally through the work of Bjerknes (1966,1969,1972). Bjerknes did more than point out the empirical relation between the two; he also proposed an explanation which requires a two-way coupling between the atmosphere and ocean in the tropical Pacific. It is fair to say that the Bjerknes hypothesis underlies all subsequent progress in understanding and modeling ENSO, though successful models of ENSO would not be possible without the rapid enhancement in our understanding of the tropical oceans and atmosphere since his time (cf Philander, 1990 and references therein). For example, the model of Zebiak and Cane (1987), discussed below, was a conscious attempt to "model" the Bjerknes hypothesis which exploits these advances to translate his ideas into suitable equations.

Bjerknes' ideas developed from observations of large-scale anomalies in the atmosphere and tropical Pacific Ocean during 1957-8, the International Geophysical Year. A major El Niño occurred in those years, bringing with it all the atmospheric changes connected to a low SOI. It is implausible that a warming confined to coastal waters off South America could cause global changes in the atmosphere, but the 1957 data showed that the rise in SST extended along the equator out to the dateline, a quarter of the earth's circumference.

Bjerknes began by recognizing a striking fact about the normal state of the tropical Pacific: the SSTs at the eastern end are remarkably cold for such low latitudes (cf especially Bjerknes 1969, from which we quote freely). Since the western Pacific is very warm, there is a large SST gradient along the equator in the Pacific. As a result there is a direct thermal circulation in the atmosphere along the equator: the relatively cold, dry air above the cold waters of the eastern

equatorial Pacific flows westward along the surface toward the warm west Pacific. “There, after having been heated and supplied with moisture from the warm waters, the equatorial air can take part in large-scale, moist-adiabatic ascent.” Some of the ascending air joins the poleward flow at upper levels associated with the Hadley circulation, and some returns to the east to sink over the eastern Pacific. There is a zonal surface pressure gradient associated with this equatorial circulation cell, high in the east and low in the west. Bjerknes named this the “Walker Circulation”, because he felt that fluctuations in this circulation initiated pulses in Walker’s Southern Oscillation. It can have such global consequences because “it operates a large tapping of potential energy by combining the large-scale rise of moist air and descent of colder dry air.”

Bjerknes also pointed out that even while the surface winds are being driven westward along the equator by the zonal SST gradient, they are acting to create the cold ocean temperatures in the east responsible for that gradient. In a search for the mechanisms responsible, differences in surface heating can quickly be ruled out: while heat flux estimates are quite uncertain, there is no doubt that more heat is going into the equatorial Pacific at the east than at the west (e.g., Weare et al., 1983; see also Bjerknes, 1969). The causes of the unusually cold SSTs are to be found in 3 features of wind-driven ocean dynamics.

(i) Horizontal advection. The easterly winds drive westward currents along the equator, advecting the cold waters from the South American coast.

(ii) Equatorial upwelling. The Coriolis force turns ocean currents to the right in the Northern Hemisphere and to the left in the Southern Hemisphere. Consequently, the surface flow at the equator is deflected poleward, and the poleward flow must be fed by waters which upwell along the equator, waters that are colder than the surface.

(iii) Upward thermocline displacement. The tropical ocean can usefully be viewed as a two-layer fluid, consisting of a warm upper ocean layer and the layer of the cold abyssal waters. In the real ocean the two are separated by the thermocline, a narrow (50-100 m) region of strong temperature change (10°C or more). The easterlies along the equator push the waters of the warm upper layer to the west, pulling the thermocline to the surface in the east. As a result the water upwelled there is colder than it would be if the upper layer waters were more evenly distributed with longitude.

The limitations of ocean theory and observation in his time made it impossible for Bjerknes to decide which of these three factors is most important (cf. Bjerknes, 1969). Even today there is considerable uncertainty as to their relative roles, although it seems to be the case that none are negligible (e.g., Seager et al., 1988).

Thus, the oceanic and atmospheric circulations over the tropical Pacific are mutually maintained by what Bjerknes (1969) referred to as a “chain reaction”; “an intensifying Walker Circulation also provides for an increase of the east-west temperature contrast that is the cause of the Walker circulation in the first place.” He also noted that the interaction could operate in the opposite sense: a decrease of the equatorial easterlies diminishes the supply of cold waters to the eastern equatorial Pacific (by any of the three mechanisms); the lessened east-west temperature contrast causes the Walker Circulation to slow down.

Bjerknes thus provided an explanation for the association of the low phase of the Southern Oscillation with El Niño as well as the association of the high phase with the normal cold state of the eastern Pacific. In each phase a positive feedback operates; in other words, an instability of the coupled-atmosphere system (Philander, et al., 1984). However, Bjerknes could not account for the turnabout from one state to the other. An explanation of the oscillation had to await 2

decades of research.

Wyrski (1975, 1979) seized on the point that during El Niño the ocean response is dynamical rather than thermodynamic (i.e., due to variations in surface heat flux). He shifted attention from SST to sea level. SST variations are readily apparent only in the eastern part of the ocean, and, as noted above, even after one recognizes that SST changes are dynamically caused, it is a far more complex response than sea level and therefore more difficult to decipher. By collecting and charting sea level data, Wyrski was able to show that the oceanic changes during El Niño are basinwide. He also showed that the initial changes in the wind were in the central and western Pacific, far from the locale of the SST changes. Finally, he suggested that the signal could propagate eastward from the area of the wind change to the South American coast through the equatorial wave guide in the form of equatorial Kelvin waves. These ideas were amplified by a number of investigators and verified in a set of numerical experiments (Busalacchi and O'Brien, 1981; Busalacchi et al., 1983). In these experiments, a landmark application of numerical modeling to ENSO research, a linear shallow water model was driven by nearly two decades of monthly surface wind stress fields. The wind forced model thermocline anomalies showed a significant correlation with sea level observations.

Two additional studies from the early 1980s stand out as foundation stones for ENSO modeling. Gill (1980) that a single vertical mode linear model could capture the major features of the tropical atmosphere's response to the anomalous heating associated with variations in tropical SSTs. Rasmusson and Carpenter (1982) synthesized the incomplete and often perplexing observational fragments into a coherent picture of the evolution of the "canonical" ENSO warm event. Though undoubtedly a simplification, this invaluable distillation provided the first specific target for models to emulate.

Though other views were (and still are) available, by the early 1980s a basis for modeling ENSO had emerged which allows much of the daunting complexity of the full atmosphere-ocean system to be ignored. The Bjerknes hypothesis is at the core of it, which means that though the consequences are global, the essential interactions between atmosphere and ocean take place in the equatorial Pacific. The variations of SST result from ocean dynamics, not variations in heat exchange with the atmosphere. Furthermore, these dynamics are essentially linear and act remotely: equatorial Kelvin waves carry the message of a wind change in the central and western equatorial Pacific eastward to effect a change in SST in the eastern Pacific. The role of the surface heat exchange is to drive the circulation of the tropical atmosphere, including the surface wind stress so crucial to the coupling. This atmospheric response can be largely captured by a steady state linear model.

3. Models of ENSO as a coupled system

A number of highly idealized coupled models were developed in the early 1980s which added significantly to our developing understanding of ENSO (see McCreary, 1985, or Philander, 1990). For example, the stability analysis of Hirst(1986, 88) provided an important vocabulary for analyzing the results of the more complex, and thus less intellectually tractable, models (also see Neelin, 1991).

The first coupled model to generate results which could be said to simulate ENSO was that of Cane and Zebiak (1985; a complete description is given in Zebiak and Cane, 1987). These non-GCM models were typically coupled systems of shallow water equations (eg Philander et al 1984; Anderson and McCreary, 1985; see the review of McCreary, 1985 or Philander, 1990 for an extended discussion). The important differences in the Zebiak and Cane (ZC) model lie

in its treatment of thermodynamics. The atmospheric heating parameterization has a moisture convergence feedback, while the ocean component includes a thermodynamically active surface layer.

The components of the ZC coupled model were developed and tested independently. The atmospheric component, described by Zebiak (1986) was shown to reproduce the major features of the equatorial wind anomaly field when forced by the composite ENSO SST anomalies (also see Weare, 1986). The oceanic component, was shown to simulate the overall evolution of SST anomalies during ENSO, when forced by observed tropical wind anomalies. [Both forcing data sets were the Rasmusson and Carpenter (1982) ENSO composites]. Both components describe perturbations about the mean climatological state, with the climatology specified from observations [specifically, the Climate Analysis Center data set; see Rasmusson and Carpenter, 1982].

a. *Atmosphere.* If SST anomalies characteristic of El Niño are given, then the principal changes in the tropical circulation may be calculated. This has been amply demonstrated by simulations with atmospheric GCM's (e.g. Shukla and Wallace, 1983; Philander, 1990). Observations show that the tropical anomalies have a simple vertical structure with a universal form, namely, a reversal of polarity between the lower and upper troposphere (e.g. regions of low level convergence lie below regions of upper level divergence). Linear dynamical models with a single degree of freedom in the vertical have proven surprisingly adept at reproducing the horizontal structure of the atmosphere though the physical interpretation of these models is uncertain (Geisler and Stevens, 1982; Zebiak, 1982; Neelin, 1989b). The ZC model dynamics is of this Gill (1980) type: i.e., steady-state, linear shallow-water equations on an equatorial beta plane. Linear dissipation in the form of Rayleigh friction and Newtonian cooling are used. The circulation is forced by a heating anomaly distribution which depends partly on local evaporation anomalies (parameterized in terms of local SST anomalies), and partly in the low-level moisture convergence (parameterized in terms of the surface wind convergence). Several observational studies (e.g., Cornejo-Garrido and Stone, 1977; Ramage, 1977) as well as GCM calculations have demonstrated the important contribution of moisture convergence to the overall tropical heat balance. The convergence feedback is incorporated into the model using an iterative procedure in which the heating at each iteration depends on the convergence field from the previous iteration. The scheme is analyzed in detail in Zebiak (1986). The feedback is nonlinear because the moisture related heating is operative only when the total wind field is convergent, and this depends not only on the calculated anomalous convergence, but also the specified mean convergence. The feedback focuses the atmospheric response to SST anomalies into or near the regions of *mean* convergence; in particular, the Intertropical Convergence Zone (ITCZ) and the South Pacific Convergence Zone (SPCZ). Such a focusing is conspicuous in the observed wind anomalies during ENSO (see Rasmusson and Carpenter, 1982).

b. *Ocean.* The model ocean basin is rectangular, and extends from 124E to 80W, and 29N to 29S. The dynamics of the model begin with the linear reduced-gravity model that is so successful in simulating thermocline depth anomalies and sea level changes during El Niño events (e.g. Busalacchi and Cane, 1985; Cane 1984). Such models produce only depth averaged baroclinic currents, but the ocean surface current is usually dominated by the frictional (Ekman) component. Therefore, a shallow frictional layer of constant depth is added to simulate the surface intensification of wind-driven currents. The dynamics of this layer are also kept linear, but only by using Rayleigh friction to stand in for nonlinear influences at the equator, a crude parameter-

ization at best. Upwelling velocity is computed as the divergence of the surface layer transport. Inclusion of a surface layer allows a strong response to local winds; models which omit it will understate upwelling effects. Monthly mean currents are generated by spinning up the model with monthly mean climatological winds. These “climatological” currents are then used in the anomaly calculation. The thermodynamics describe the evolution of temperature *anomalies* in the model surface layer. The governing equation is complete, including three-dimensional temperature advection by both the specified mean currents and the calculated anomalous currents. As noted above, the evidence is that surface heating does not contribute to the El Niño warming. Instead, the data indicate an inverse relation between SST and heat flux into the ocean because of increased evaporation. In the model, surface heat flux anomaly is taken to be proportional to the local SST anomaly, acting always to adjust the temperature field toward the climatological mean state. This (monthly) mean temperature structure is specified from observations. The thermodynamic equation thus has the following form (where barred quantities represent mean fields and unbarred quantities represent anomalies):

$$\frac{\partial T}{\partial t} = -\bar{\mathbf{u}}_1 \cdot \nabla T - \mathbf{u}_1 \cdot \nabla (\bar{T} + T) - \{M(\bar{w}_s + w_s) - M(\bar{w}_s)\} \bar{T}_z - M(\bar{w}_s + w_s) T_z - \alpha_s T, \quad (1)$$

where \mathbf{u}_1 and w_s represent horizontal surface currents and upwelling, respectively, and the function $M(x)$ is defined by $M(x) = x$ for $x > 0$ and $M(x) = 0$ otherwise. This function accounts for the fact that surface temperature is affected by vertical advection only in the presence of upwelling. The anomalous temperature gradient, T_z , is defined by

$$T_z = (T - T_e)/H_1, \quad (2)$$

where H_1 is the surface layer depth, and the T_e measures anomalous temperature of the waters entrained into the surface layer. This water, at the base of the mixed layer, is a mixture of the surface water and the unperturbed waters below. Hence

$$T_e = (1 - \gamma)T + \gamma T_d$$

where γ ($= .5$) is a mixing parameter and $T_d(h, \bar{h})$ relates the subsurface temperature anomaly to the mean and anomalous thermocline depths. It is essentially a curve fit to the equatorial vertical temperature profile (in addition to Zebiak and Cane (1987), see Seager et al., (1988). The variable h is obtained from the model dynamics.

c. *Coupling.* In the component models, the ocean affects the atmosphere exclusively through the SST field, and the atmosphere affects the ocean through the surface wind stress alone. Though it was reasonable to consider a steady-state atmosphere when prescribing seasonal mean SST forcing (as in Zebiak, 1986) this must be reconsidered when coupling to a time-dependent ocean in which the SST field can change on the timescale of a few days. For boundary forcing variations on this timescale, the atmospheric response due to moisture convergence feedback cannot reasonably be assumed to be in continuous equilibrium, since the transport time between regions of moisture input and corresponding latent heat release during ENSO can easily approach one month. This is an important consideration for the coupled model. If the atmospheric response is assumed to be in continuous equilibrium, then the *change* in the wind field between successive SST time steps will be overestimated. As a result, more rapid

changes in SST will occur because of local wind effects. This induces yet larger changes in the atmosphere, and the combined interaction favors an artificially rapid development of anomalies, particularly at small scales where the atmospheric convergence feedback is most efficient. To circumvent this, a procedure was adopted which effectively gives the steady-state response as before for timescales of one month or more, but restricts the feedback for shorter timescales. This is accomplished by altering the criterion governing the number of convergence feedback iterations that are performed. Other methods could be used to produce a similar result. For example a spatial smoother could be applied after each iteration, or time dependence could be added explicitly to the atmosphere model. The present method was chosen because it requires less computation.

d. *Numerical methods* The numerical procedure used to solve the atmospheric component model is given in the appendix to Zebiak (1982). The dynamical equations are solved on an equatorial beta plane in a manner which mimics the usual derivation of equatorial waves: variables are first Fourier transformed in x , then the operator resulting from a finite difference approximation in y is inverted for each zonal wave number to obtain the meridional velocity v , after which the other model variables are obtained from expressions in terms of v . Details of the ocean solution procedure are given in Zebiak and Cane (1987; also see Blumenthal and Cane, 1989). The baroclinic flow governed by the linear shallow water equations is solved for by the method of Cane and Patton (1984). Employing a filtered model with only the Kelvin and long Rossby waves explicitly calculated leads to a very efficient implicit scheme which allows a 10 day timestep.

e. *Coupled model results.* A numerical experiment with the coupled model was initiated with an imposed 2 m/s westerly wind anomaly of four months duration. There was no external forcing thereafter: aside from the model physics, evolution of anomalies in SST, winds, etc depends only on this initial condition and on the monthly mean climatological fields specified in the component ocean and atmosphere models. Furthermore, because of the damping in the model the initial conditions are largely forgotten within a decade. A time series of model SST anomaly averaged over the eastern equatorial Pacific is shown in Fig. 1a. There are peaks of varying amplitude occurring at irregular intervals but typically 3 to 4 years apart. They tend to be phase-locked to the annual cycle, with major events reaching maximum amplitude at the end of the calendar year and decaying rapidly thereafter. All of these features are characteristic of observed El Niño events. The amplitude of model events is similar to observed ones. The model appears to be somewhat more regular than nature; the high frequency fluctuations present only in the real atmosphere and ocean may account for the broader natural spectrum (but see below). Fig. 2 depicts the evolution of SST during a typical El Niño event. In December of the preceding year, not shown there was no discernible anomaly; by March of the El Niño year there is a small but systematic warming in the eastern Pacific; by December the anomaly extends to the dateline, with a maximum at about 135°W . Figs. 3 and 4 show the first 4 EOFs of model and data, respectively. The 4 model EOFs account for a higher percentage of the variance than the 4 observed EOFs. Since all the higher EOFs have only a small part of the variance, this remainder may all be regarded as noise, and it is to be expected that the full, natural system will be noisier than the ENSO specific model. The variance distribution shows that the 2nd, 3rd and 4th modes are relatively more significant in nature, corresponding to the fact that nature exhibits more propagation within an event, and more differences from event to event. The correspondence between the model and observed structures is obvious enough to permit the assertion that the

model is realistic, though there are important discrepancies. That the model understates the strength of the signal at the South American coast is likely due to its coarse resolution, which precludes a decent simulation of coastal upwelling. The model's systematic understatement of the variability westward of about 160W is a shortcoming with more serious consequences.

Fig. 5 illustrates the evolution of zonal wind along the equator. The prominent feature is the band of westerly anomalies in the central Pacific. It resembles the typical ENSO anomaly (Cane, 1983) but lacks the observed eastward progression in its early stages. What is missing is the initial anomaly west of the dateline. The model atmosphere has no SST anomaly to respond to, because the ocean model has too little variability there. Thereafter, the spatial and temporal patterns are generally realistic until the year following the event, year 32. The model westerly anomalies persist several months longer than is typical of El Niño events. The same is true for SST and other fields, and is characteristic of model events. A possible cause is the model's inability to produce the easterly anomalies in the far western Pacific which appear during the termination phase of observed events. As is the case even when observed SST anomalies are specified, the model winds are poorest in the Asian Monsoon region and in the far eastern Pacific. As with observed events, El Niño anomalies disappear quite rapidly, to be replaced by cold SST in the eastern Pacific and stronger than normal easterlies along the equator.

In summary, the coupled ocean-atmosphere model, which greatly simplifies the physics of the real ocean-atmosphere system and is certainly unrealistic in many details, nonetheless reproduces the most prominent spatial and temporal features of the evolution of El Niño events. Mechanisms internal to the model allow it to terminate events and initiate new ones in a never-ending ENSO cycle.

Battisti (1988) coded a version of the ZC model which also captures many of the features of the observed ENSO. However, it fails to exhibit the aperiodic behavior which generally obtains in the original ZC model. The Battisti version behaves as though it is more dissipative, but the reasons for this are not understood. Battisti and Hirst (1989) were guided by experiments with this model in developing a paradigm for the ENSO mechanism (see below).

A coupled ocean-atmosphere oscillation was also achieved (Fig. 6) in the more complex model of Schopf and Suarez (1988). The ocean component was documented in Schopf and Cane (1983). It covers the tropical Pacific only, and has almost the same vertical structure as the ZC ocean, with 2 active layers above a motionless abyss. However, the physics is more comprehensive. Dynamics are governed by the primitive equations and the temperature of the lower active layer is predicted within the model. The depth of the surface layer is variable, affected by surface divergence and by mixed layer physics of the Kraus-Turner type (Kraus and Turner, 1967; Schopf and Cane, 1983).

The atmospheric model is a finite difference version of the 2 level primitive equation model of Held and Suarez (1978). Its atmospheric physics parameterizes radiative processes by a relaxation to a specified zonal mean temperatures. It includes dry, but not moist, convective processes. The coupled run is forced by mean annual radiation; there is no seasonal cycle.

The Bjerknes-Wyrski theory lacked an explanation for the perpetual turnabout from warm to cold states and back again. While the explanation is inherent in the physics outlined in the previous section, it did not emerge until after the development of the numerical models described above. Though later described in very simple systems such as a single ODE with a delay (Suarez and Schopf, 1988; Schopf and Suarez, 1990; Battisti and Hirst, 1989) or a recurrence relation (Cane et al 1990; Münnich et al 1991), this theory is properly regarded as

one of the fruits of numerical modeling.

As in nature, let the main wind changes be in the central equatorial ocean while the SST changes are concentrated in the east. Then the surface wind amplitude, which depends on the east-west temperature gradient, varies with this eastern temperature. Further simplify by assuming that this eastern SST is principally controlled by thermocline depth variations. These variations are driven by the changes in the surface wind stress according to the linear shallow water equations on an equatorial beta plane. If the eastern SST is warm (thermocline high) then the wind anomaly will be westerly, forcing a Kelvin wave packet in the ocean to further depress the thermocline in the east thus enhancing this state.

However, this excess of warm water must be compensated somewhere by a region of colder water (shallower than normal thermocline). Equatorial dynamics dictates that this be in the form of equatorial Rossby wave packets, which must propagate westward from the wind forcing region. When they reach the western boundary they are reflected as “cold” equatorial Kelvin waves, which propagate eastward across the ocean to reduce the SST there. Thus the original warm signal is invariably accompanied by a cold signal – but with a delay. This delayed oscillator mechanism accounts for the turnabout from warm to cold states. The wraparound Hovmuller diagram of Fig. 7 illustrates this in the model of Schopf and Suarez (1988).

It is especially relevant to the prediction problem to consider the state of affairs when the eastern thermocline and SST anomalies are near zero; for example, at the termination of a warm event. Then the wind anomaly must be near zero as well, so there is no direct driving to evolve the coupled system to its next phase. However, the previous warm event necessarily left a residue of cold Rossby waves in the western ocean, which eventually reflect at the west into a Kelvin wave which will reduce the SST in the east. The wind then becomes easterly and the cycle continues. The clear implication is that knowledge of the state of the ocean thermocline is essential to predicting the system’s future behavior.

The cause of the observed aperiodicity remains an unsettled issue. The results from Battisti’s (1988) model and the experiments of Schopf and Suarez (1988) suggest that it is due to noise; that is, atmospheric or oceanic fluctuations distinct from the ENSO cycle. On the other hand, the low order ENSO model of Münnich et al (1991) produces aperiodicity, doing so rather readily if a seasonal modulation is included. Regardless of the reason for it, aperiodicity does exist in nature, and so the predictability of ENSO is limited.

This complicates attempts to verify ENSO models: even a perfect model can’t reproduce the time evolution of the observed cycle for very long. (The same problem arises for all climate models.) Short sequences on the order of a year may be verified; this is the prediction problem discussed in the next section. Another test is to ask whether the model’s characteristic variability is “realistic”. Zebiak and Cane (1989) assayed an answer by comparing a number of statistics from model generated eastern Pacific (NINO3) SST time series with those calculated from observed time series. In this study 243-100-year long model runs were made in which each of 5 model parameters were given one of 3 values: unchanged from the values in the standard run (ie the run depicted in Fig. 1a; cf Zebiak and Cane, 1987 for a description of model parameters), increased by 5%, or decreased by 5%. The large number of runs allow one to conclude with (statistical) confidence that these modest changes in parameter values altered the characteristic amplitude and frequency of events, as well as the degree of irregularity of the oscillations. In most cases aperiodic oscillations with an average period near 4 years still occur. One may make subjective judgements as to the relative reality of difference parameter settings, but the short

length of the observed NINO3 record (18 years) only allowed a small number of cases with obviously pathological behaviors to be confidently labeled "unrealistic".

Zhao et al (1991) were able to reach a more definite conclusion by comparing with a 500 year record of accumulation from the Quelccaya ice-cap in Peru. Best agreement with the statistical characteristics of this record were obtained by decreasing the oceanic equivalent depth and increasing the sharpness of the thermocline while reducing its overall amplitude. As above, changes are 5% variations from the standard run. The earlier study showed that, taken by itself, the equivalent depth change would tend to increase event amplitude while decreasing their frequency. Decreasing thermocline amplitude had the opposite effect on event amplitude and enhanced the preference for a 4 year period. The only apparent effect of the change in thermocline sharpness is to decrease the amplitude of the very large events.

The model calculates only anomalies, and the parameter changes are equivalent to changes in the mean background state. Since a greenhouse warming will alter this state, the implication of the parameter sensitivity study is that characteristics of ENSO will be changed. Fig. 1b resulted from a scenario which simplistically assumes a uniform 1°C warming of the atmosphere and ocean. The most important effect for ENSO is an increase in the latent heat flux. Fig. 1 shows that events are larger and more regular than in the standard case.

Results from a more elaborate alternate scenario are shown in Fig 8. In addition to the 1C temperature increase, a 5% increase in specific humidity is also assumed. This alters the heat flux into the ocean, and increases the surface convergence of moisture and hence atmospheric heating. The expectation that the warming will be greater at higher latitudes (eg Hansen et al 1988) suggests that the waters feeding the equatorial thermocline will warm more than the surface. Hence the near-surface stratification is decreased. Fig. 8 shows the ENSO cycle to be more irregular and less energetic. A new behavior appears: multi-decadal sequences of continuously warm SST anomalies. The experiments based on these crude scenarios cannot be seriously regarded as predictions. They merely hint at possible changes in interannual variability.

4. Prediction by dynamical models (and other methods) Its social and economic benefit makes prediction a principal goal of climate modeling. Attempts at prediction also provide an objective and quantitative measure of our collective scientific understanding and modeling skill.

Dynamical models are the method of choice in weather forecasting. Thus far ZC is the only dynamical model used for forecasting ENSO. Procedures and results are described in Cane et al (1986), Cane and Zebiak (1987), Barnett et al (1988) and Cane (1990). Other than climatology, the only data input into the model is surface wind stress anomalies. The ocean component of the coupled model is forced over time by these fields to create fields of SST, currents and thermocline displacements. The atmosphere component is then forced by this model SST to create a wind field. This procedure creates a complete set of internally consistent coupled model initial conditions, albeit ones which do not agree with observations. From the initial time onward the coupled model is run forward with no further inputs.

The first forecasts with the ZC model were made in 1985, and the prediction of a warm even for late 1986 was published in early 1986 (Cane et al 1986). Fig 9 compares this forecast's SST field with observations for January 1987. The forecast is clearly correct in indicating a moderate amplitude warm event. Note that the major discrepancies in the predicted pattern are the same as those revealed in Figs. 3 and 4. A more important error was the early start to the predicted warming (see Barnett et al 1988 and Figs 10 and 12), another systematic model problem.

Fig. 10 shows illustrates the forecast performance at various leads in terms of the eastern

equatorial Pacific SST index, NINO3. Since the initial conditions do not use observed SST, the initial model SST may also be compared with data. The major events are captured at leads out to a year, with few false events other than the consistent tendency to persist the 1982-83 event. Even the 2 year lead captures much of the observed behavior. At all leads, including 0, the model is better at forecasting the major departures from normal (ie the events) than at tracking the smaller amplitude higher frequency fluctuations. The impression that the 3 month lead is only slightly worse than the initial conditions, and that the falloff in skill is slow from 6 months to a year is confirmed in Fig. 11. This summary masks a marked seasonal dependence, with model skill being greatest for boreal fall and winter (eg Cane, 1990 Fig.11.5).

Statistical models have also been used to forecast ENSO. Graham et al (1987a,b) present a scheme for forecasting SST using wind fields as the short term predictor and atmospheric surface pressure at leads beyond a season. As with the dynamical model the skill is in capturing the major events, not the smaller fluctuations. Barnett et al (1988) evaluated the 1986-87 forecasts of this scheme, the ZC dynamical forecasts, and a statistical- dynamical scheme due to Inoue and O'Brien (1984). This paper also demonstrates how the statistical model may be used to enrich our understanding of the evolution of ENSO events. Fig. 12, from Barnett et al (1988), shows the performance of the statistical and dynamical models to be roughly comparable, with the statistical model doing better at short range and the dynamical one doing better at longer leads. This seems to be a systematic difference, although the samples are too small to be conclusive and the regions forecast for are not identical. Both models show the same seasonal dependence in skill; note in Fig. 12 that the statistical model's forecasts in the low skill summer season are judged not to be statistically significant.

Xu and von Storch (1990) describe an interesting statistical forecast procedure in which the data is fit to a first order Markov process. The objects forecast are the eigenfunctions of this Markov model, referred to as Principal Oscillation Patterns or POPs. It turns out, not at all fortuitously, that the leading POP is obviously an ENSO mode. The performance of this model is indicated by Fig. 13 (however, note that this is hindcast skill). Comparison with the dynamical model results of Fig. 11 shows this model has higher skill at short leads and lesser skill at long leads. The data used in the POP model is South Pacific winds fields, data apparently contributing little or nothing to the skill of the other schemes.

The skill of ENSO forecasts, whether statistical or dynamical, is not high. Nonetheless, they offer considerable grounds for optimism. Still in their infancy, they have already established that important aspects of ENSO are predictable at lead times of several seasons. Useful forecasts have been achieved even while our understanding of the phenomena is incomplete and the data for a full set of initial conditions (or statistical predictors) is largely unavailable.

Issues limiting predictive skill fall in 3 categories: intrinsic limits to predictability; inadequate data; model shortcomings. The 3 interact in a forecast, and the period of usable data is short relative to the timescale of the events, so it is difficult to establish their relative importance for forecast error. There have been only a few studies of ENSO predictability (Goswami and Shukla, 1991; Blumenthal, 1991; Latif et al 1991), but it seems likely that at this primitive stage the latter 2 categories account for limits to present skill.

The sizable gaps in the data over the tropical Pacific are notorious (Reynolds et al, 1989 is but one example), but the efforts of the TOGA program are effecting a marked improvement. The lack of data and the fact that little is usable before the mid 1950s limits the possible complexity of statistical models. Only a model with a small number of predictors can be validated.

All the statistical models used to date are linear; nonlinear methods will be especially difficult to apply in the face of these data difficulties.

Techniques of data assimilation are well known in numerical weather prediction, and this is currently a very active research area. While relatively little has been done in oceanography (see the review by Ghil and Manolette-Rizzoli, (1990) there are a few rather sophisticated applications of data assimilation to tropical ocean GCMs (Derber and Rosati, 1989; Leetmaa and Ji, 1989). Application to coupled models is just beginning; note that the ZC efforts have yet to use any oceanographic data.

The fact that the ZC model is far less comprehensive than coupled GCMs is a didactic advantage. Among its many simplifications of reality, it virtually ignores the world beyond the tropical Pacific, and omits much of the physics important for fluctuations on time scales shorter than a few months (cf Seager, 1989; Zebiak, 1990). Its forecasting performance builds confidence in the essential correctness of the theory for ENSO outlined previously. In particular, it supports the Bjerknes hypothesis, with its the emphasis on large scale ocean -atmosphere interactions in the tropical Pacific. The statistical methods lend added support to the essence of ENSO being large scale and low frequency, but they do use predictors outside the equatorial Pacific. By its construction, the ZC model also argues for the primacy of linear dynamics, relegating the important nonlinearities to the thermodynamics. If the active SST changes are east of the wind changes then linear equatorial dynamics make the delayed oscillator mechanism inevitable.

5. Coupled GCMs

The previous discussion points to the desirability of a comprehensive ENSO model – a coupled GCM (CGCM). Beyond the ENSO perspective, there is the need for a comprehensive climate system model which, while able to simulate ENSO and other natural climate variability, also contains the physics to respond correctly to changes in greenhouse gases. Not only is a detailed review of all the ENSO CGCMs impossible here, but the rapid ongoing progress ensures that it would soon be dated. A recent compendium of ENSO results from 17 coupled models (Neelin et al, 1991) is available to speed this progress; it should be consulted for the broadest status report on ENSO modeling at this time (early 1991).

The successes of the intermediate models establish that the physics needed to produce a reasonable ENSO cycle is known and can be modeled. Our ability to construct an ENSO CGCM is thus demonstrated in principle. Practice is another matter. In the less elaborate parameterizations of the simpler models the effects of changes in parameter values are more apparent; ie these models are easier to tune. Their relative simplicity makes them easier (if not always easy) to understand. That these models are fast enough to run many times per GCM experiment compounds these advantages. Striving for a complete test of our understanding of the climate system, the GCMs try to assume as little as possible. The intermediate models with their limited goals are willing to specify a great deal. For example, in the ZC model the mean climatology is taken from data as is the subsurface temperature structure.

CGCM ENSO work generally has not followed the path of numerical weather prediction, which progressed over time from the equivalent barotropic vorticity equation to increasingly more complex models. Instead, existing "state of the art" atmospheric and oceanic GCMs have been coupled together. For subtle reasons, this approach has proven more frustrating than anticipated.

It is usual practice before coupling to test the component models independently by specify-

ing climatological forcing (ie SST for the atmosphere GCM, surface wind stress, salt and heat flux for the ocean GCM), in order to see if they produce a reasonable climatology. In some cases they have also been forced with anomalies observed in ENSO years. Few, if any, of these climate models have been compared with observations in anything like the quantitative manner of weather prediction models. "Reasonable" is not a precise standard and need not be rigorous; in some cases the ensuing troubles may be due to excessive leniency.

A GCM may do a good job overall while doing poorly on a feature crucial for the ENSO interaction. For example, atmospheric GCMs, even those with excellent simulations of surface pressure, 500 mb height, etc, typically understate the strength of tropical surface wind stress. By a global measure the model surface wind may be quite good, but the equatorial winds count disproportionately for ENSO. In a simple model one might just crank up the surface drag coefficient and use the higher stress to drive the ocean. Atmospheric GCMs tend to counter an increased drag coefficient by reducing the surface wind, leaving the stress almost the same.

Let us assume that an atmosphere and ocean GCM are each capable of a reasonable simulation of climatology. Beyond what inferences may be drawn from our understanding of ENSO, we have few notions of how reasonable they must be before the coupled model will produce a satisfactory ENSO cycle. Only experience can tell us. The lesson of experience has been that coupling 2 reasonable GCMs most often causes their flaws to feedback on each other, moving the model climate system far from reality, a result known as "climate drift".

A well analyzed example is provided by the UCLA experience, as described in Neelin et al (1991), from which we quote below. The sophisticated UCLA atmospheric GCM is coupled to the GFDL tropical Pacific model, the most thoroughly studied of ocean GCMs. Excessive surface heating in the southern hemisphere increases the near surface stability in the ocean, causing the Richardson number mixing parameterization (Pacanowski and Philander, 1981) to reduce turbulent heat fluxes out of the surface layer to the ocean below. The warm SSTs pull the ITCZ south of the equator in the warm season. The incorrect wind pattern further contributes to the warming. "The interaction of the GCM fluxes with the vertical mixing parameterization thus apparently sets off a whole chain of coupled processes which result in a climatic state departing significantly from the observed. However, uncoupled tests did not reveal anything obviously wrong with either of these parameterizations. In hindsight, the mixed layer depth in the subtropics ... does tend to be too shallow."

This example seems to support the conventional wisdom that the ocean GCMs are the weak link; atmospheric GCMs have a much longer and richer history. Vertical mixing is one of the most uncertain parameterizations, but the surface layer deficiencies of the Pacanowski and Philander (1981) scheme are becoming well known and can be remedied readily (eg Philander et al, 1987; Sec 2b of Neelin et al).

In fact, surface wind stress and surface heat flux, the only aspects of the atmosphere which matter in driving the ocean, are not well simulated by GCMs. Among other things, both depend strongly on the parameterization of the planetary boundary layer, not one of the strongest features of these models. Since these surface fluxes of heat and momentum matter little for weather prediction or for any other atmospheric model run with specified SSTs, they were long neglected. This has changed only recently with the heightened interest in modeling the coupled system, ENSO in particular. A recent comparison of the operational NMC surface wind analysis with tropical Pacific buoy data (Reynolds et al, 1989) shows that despite great progress, even the best of GCMs need improvement.

The heat flux is an even more difficult problem. It shares with wind stress the uncertainties in parameterization of surface turbulent fluxes (eg Blanc, 1987). In addition, it depends on the radiation balance, which in turn depends on cloud-radiative interactions, one of the greatest uncertainties in GCMs. Since the climatological heat balance is poorly known, it is difficult to calibrate heat flux models directly. (Seager et al, 1988 calibrate indirectly on SST via an ocean model.) Even relatively small errors can be unacceptable. Weare et al (1981) estimate the heat flux errors to be about $30W/m^2$, enough to heat a 50m mixed layer by $4^{\circ}C$ in a year. In the western equatorial Pacific, where the SST varies by only $1C$ in a year a systematic error of $7W/m^2$ would make difficulties.

The conclusion is that the ocean GCMs, young and flawed as they are, do their job of delivering reasonable tropical SSTs at least as well as the atmospheric GCMs do their more difficult job of delivering acceptable wind stresses and heat fluxes. (The best known shortcomings of ocean GCMs, such as not enough deep water formation, incorrect separation point for the Gulf Stream are irrelevant to ENSO.) The CGCM flaws, wherever they lie, make it necessary to compensate for climate drift by a "flux correction" (for such a young business CGCMs have sure piled up the jargon): the surface fluxes are modified to produce a good climatology. The fluxes out of the ocean no longer need be consistent with those going into the atmosphere; also, flux correction can inhibit interannual variability even while it fixes the climatology (Latif et al 1988b). An apparent alternate solution to the climate drift problem is to formulate the model as an anomaly model, as with ZC. But since every flux correction procedure can be formulated as an equivalent anomaly model, the two approaches are not distinct. The most satisfactory solution is to correct the deficiencies.

One strategy which recognizes the problems and computer time demands on the atmospheric side is to construct a hybrid by coupling a simple atmospheric model to an ocean GCM. Latif et al (1991) constructed an empirical atmosphere model from statistical relations between SST and surface wind which was coupled to a GCM and used in prediction studies. Their results are at least comparable to the statistical prediction techniques. Neelin (1990) used a hybrid model to good advantage to study the changes in behavior with changes in mean climatology and in the "coupling strength", ie the amplitude of the wind anomaly for a given SST anomaly. The model climatology can be readily adjusted by a flux correction technique. It was found that a mean state with an excessive cold tongue inhibited interannual variability, but a more realistic state allows it (Fig. 14). This perfectly periodic oscillation has power at 2 periods: just under 4 years and 5-6 months.

In all the true CGCMs the atmospheric GCM is too coarse (usually R15 or T21) to resolve all the significant features of the tropical atmosphere, most notably the ITCZ. For many of the CGCMs, especially those intended for global climate studies rather than ENSO, the ocean GCM is also low resolution, typically 4×5 degrees of latitude and longitude. This is too coarse to simulate equatorial wave dynamics properly, and makes equatorial upwelling far too weak. Thus the models are unable to capture some of the most essential features of equatorial oceans, features which were also central to the ENSO paradigm presented above. As a rule, the zonal SST gradient along the equator is too weak in these models. In some the the minimum temperature is at the center of the basin or the gradient is reversed relative to observations. (Neelin et al 1991 and Meehl 1990b review most of these coarse ocean CGCMs.)

Nonetheless, a number of these coupled simulations exhibit interannual variations with the 3 to 4 year timescale characteristic of ENSO. Fig. 15, from Meehl (1990a) is an example. It

is typical in that the anomalies are 1C or less, much weaker than the observed ENSO. They invariably propagate westward. Neelin (1991) identifies them as "SST modes", instabilities involving a two-way coupling between SST and the atmosphere, but without a role for the wave dynamics central to the paradigm presented above.

A number of the half dozen or so CGCMs with high resolution ocean components give reasonable climatologies (Neelin et al 1991 describes all these CGCMs), but to date only one exhibits interannual variability with amplitudes comparable to the observed ENSO (Philander et al, 1991). The response of the atmospheric component, the GFDL R15 climate model, to observed SST anomalies has been described by Lau (1985). The ocean model climatology is described by Philander et al (1987). There is no flux correction. Annually averaged solar insolation is applied; there is no seasonal cycle.

The evolution of SST for a 28 year run is shown in Fig. 16. The mean SSTs are a bit warm, but are reasonably close to observed values. The anomalies tend to be stationary, with realistic amplitudes and patterns. However, they tend to persist for about 3 years, roughly twice the length of observed events. The absence of an annual cycle may account for some loss of realism. The results of this simulation, especially the temporal variations in heat content, suggest the equatorial wave mechanism discussed above as an appropriate explanation for the oscillation (cf Neelin et al, 1991; Philander et al, 1991).

In the simulation shown the clouds were held fixed at climatological values. Two additional runs were made with interactive clouds. The first went into a perpetual warm state – a permanent El Niño. In the second the solar constant was reduced by 10additional reminders of the sensitivity of CGCMs to parameter variations and changes in model formulations.

6. Discussion

As we begin to model the complete climate system, it is encouraging that enough success has been achieved in modeling a complex subsystem to permit skillful forecasts a year in advance. In somewhat less than 5 years, we progressed from having no models capable of a reasonable phenomenological simulation to having a dynamical forecast model of some practical value.

At the same time, the history we have reviewed here is grounds for some pessimism. The skill and precision of the forecasts is still quite limited. It has proven far more difficult than anticipated to achieve realistic simulations of ENSO by coupling comprehensive state-of-the-art general circulation models (GCMs). The coupled system stresses model weaknesses which appeared unimportant when the components were run separately.

ENSO modeling began with a fairly specific goal, to simulate the observed cycle . It could be built on sound physical ideas developed from insightful analyses of an inadequate data set. Despite the apparent realism and immediate availability of GCMs, the earliest successes were achieved with less comprehensive models designed to capture the physics singled out by the early hypotheses. But modeling success did not have to wait for a complete theory. In fact, the models were instrumental in extending the theory.

One of these intermediate models proved able to forecast ENSO with some skill a year or more ahead. This is surprising in view of the many features of the atmosphere and ocean it is unable to reproduce. Together with the statistical model performance, it supports the concept that the interactions shaping this primary feature of natural variability in the climate system have large space and time scales (cf Barnett et al 1988). It can be pushed further, to suggest that the core interaction is too robust to be disturbed by the myriad factors ignored (smaller time and space scales, land processes, biology, etc). Probably this is pushing too far: it is likely that

some of those factors do influence the evolution of ENSO, so a prediction model which cannot simulate them is handicapped.

However, this is not proven and it is not inevitable. It could be that other factors which influence ENSO are themselves unpredictable, so a model able to simulate them will have no greater forecast skill. (Midlatitude synoptic systems are a well known example of features unpredictable on the seasonal and longer lead times of interest for ENSO.) A corollary is that the existence of such influences would make ENSO less predictable.

To generalize, when the predictability of climate features is inherently limited, it may be that nothing is to be gained by building a more inclusive model. The best to be done is a statistical description of possible futures. A thorough simulation of such features may be unproductive, but some consideration of their influence (ie a parameterization) is still needed. This is absent in present intermediate models for ENSO.

Intrinsic loss of predictability is probably not the principal impediment to better forecasts. At this early stage, the crudeness of the coupled model renders it incapable of simulating important low frequency large scale aspects of the tropical Pacific, let alone the rest of the global system. Improvements are well within reach, which is grounds for believing the forecasts can be improved. Another limit is imposed by the poor quality and coverage of the data. It is hard to say how much of the mediocre forecast performance is attributable to poor initial conditions and how much to model flaws. The expansion of the ocean observing system accomplished by the TOGA Program will go a long way toward reducing the data problems. Though the level of skill ENSO forecasting can attain in the immediate future is far from clear, there are solid reasons for optimism.

Whatever the causes, the limited intrinsic predictability of ENSO phenomena complicates attempts to verify models. Short simulations (predictions) may be directly compared with data, but not long time behavior. Verifying statistics of model variability demands very long time series.

All of the same issues arise for climate system models. It is even more difficult to validate models intended to predict the consequences of changes which have no past precedent. A necessary, but hardly sufficient, requirement for a greenhouse climate model is an ability to simulate ENSO. Illustrations (Figs 1 and 9) offered above are reminders that changes in interannual variability are a possible consequence of increases in greenhouse gases.

The relatively simple models first used for numerical weather prediction were consciously built on the basis of existing observational and theoretical understanding (eg equivalent barotropic structure; baroclinic instability rather than thermodynamics as the cause of synoptic systems). Computer time was an important constraint, but so was the limited understanding of how to make a complex model work. It took 2 decades before operational forecasts were made with GCM class models.

GCMs existed at the outset of ENSO modeling, so it was possible to try to skip ahead to a CGCM rather than building up to it slowly. Nonetheless, it turned out that the practice of ENSO modeling tended to recapitulate the history of NWP. GCM efforts are again constrained by limits on understanding and computational resources. The latter forces insufficient resolution to resolve the important physics. The intermediate models have the developmental advantage of hundreds and thousands of simulated years of experiments; the GCMs cannot afford to follow suit. Limits to understanding are brought into relief by coupling experiments. Physical parameterizations which seemed adequate in uncoupled mode become crippling. Coupling ocean and

atmosphere GCMs sorely tries physics which was safely neglected in previous modeling work.

The difficulties do not diminish the desirability of a CGCM. The simpler models demonstrate it can be done, and provide some valuable guidance on how to do it. The often exquisite parameter sensitivities of CGCMs (Neelin et al, 1991) notwithstanding, the demonstrated ability of at least one CGCM to generate realistic interannual variations is enormously encouraging. It seems altogether likely that satisfactory ENSO CGCMs will follow the first model successes in less than a decade, rapid progress in such a complex task.

References

- [1] D. L. T. Anderson and J. P. McCreary, *Slowly propagating disturbances in a coupled ocean-atmosphere model.*, J. Atmos. Sci. **42** (1985), 615–629.
- [2] T. P. Barnett, N. Graham, M. A. Cane, S. E. Zebiak, S. Dolan, J. J. O’Brien, and D. Legler, *On the prediction of the El Niño of 1986-1987*, Science **241** (1988), 192–196.
- [3] D. S. Battisti, *The dynamics and thermodynamics of a warming event in a coupled tropical atmosphere/ocean model.*, J. Atmos. Sci. **45** (1988), 2889–2919.
- [4] D. S. Battisti and A. C. Hirst, *Interannual variability in the tropical atmosphere/ocean system: influence of the basic state and ocean geometry*, J. Atmos. Sci. **46** (1989), 1687–1712.
- [5] J. Bjerknes, *A possible response of the atmospheric Hadley circulation to equatorial anomalies of ocean temperature.*, Tellus **18** (1966), 820–29.
- [6] ———, *Atmospheric teleconnections from the equatorial Pacific*, Mon. Wea. Rev. **97** (1969), 163–72.
- [7] ———, *Large-scale atmospheric response to the 1964-65 Pacific equatorial warming*, J. Phys. Oceanogr. **15** (1972), 1255–73.
- [8] T. V. Blanc, *Accuracy of bulk method determined flux, stability, and sea surface roughness*, J. Geophys. Res. **80** (1987), 3867–3876.
- [9] M. Benno Blumenthal, *Predictability of a coupled ocean-atmosphere model*, J. Climate **4** (1991), no. 8, 766–784.
- [10] M. Benno Blumenthal and Mark A. Cane, *Accounting for parameter uncertainties in model verification: an illustration with tropical sea surface temperature*, J. Phys. Oceanogr. **19** (1989), 815–830.
- [11] A. J. Busalacchi and Mark A. Cane, *Hindcasts of sea level variations during 1982/83 El Niño*, J. Phys. Oceanogr. **15** (1985), 213–221.
- [12] A. J. Busalacchi and J. J. O’Brien, *Interannual variability of the equatorial Pacific in the 1960s*, J. Geophys. Res. **86** (1981), 10901–10907.

- [13] A. J. Busalacchi, K. Takeuchi, and J. J. O'Brien, *Interannual variability of the equatorial Pacific - revisited*, *J. of Geophys. Res.* **88** (1983), 7551–7562.
- [14] T. Y. Canby, *El Niño's ill wind*, *Natl. Geogr.* **165** (1984), 144–183.
- [15] M. A. Cane, *El Niño*, *Ann. Rev. Earth Planet Sci.* **14** (1986), 43–70.
- [16] ———, *Forecasting El Niño with a Geophysical Model*, *Teleconnections Linking World-wide Climate Anomalies*. (M. H. Glantz, R. W. Katz, and N. Nicholls, eds.), Cambridge U. Press, Cambridge, England, 1991, pp. 345–369.
- [17] M. A. Cane, M. Münnich, and S. E. Zebiak, *A Study of Self-Excited Oscillations of the Tropical Ocean-Atmosphere System. Part I: Linear Analysis*, *J. Atmos. Sci.* **47** (1990), 1562–1577.
- [18] M. A. Cane, S. E. Zebiak, and S. C. Dolan, *Experimental forecasts of El Niño*, *Nature* **321** (1986), 827–832.
- [19] Mark A. Cane, *Oceanographic events during El Niño*, *Science* **222** (1983), 1189–1194.
- [20] ———, *Modeling sea level during El Niño*, *J. Phys. Oceanogr.* **14** (1984), 586–606.
- [21] Mark A. Cane and R. J. Patton, *A numerical model for low-frequency equatorial dynamics*, *J. Phys. Oceanogr.* **14** (1984), 1853–1863.
- [22] Mark A. Cane and S. E. Zebiak, *A theory for El Niño and the Southern Oscillation*, *Science* **228** (1985), 1085–1087.
- [23] ———, *Deterministic prediction of El Niño events.*, *Atmospheric and Oceanic Variability* (H. Cattle, ed.), Royal Meteorological Society/American Meteorological Society, 1987, pp. 153–182.
- [24] Cornejo-Garrido and P. H. A. G. Stone, *On the heat balance of the Walker Circulation*, *J. Atmos. Sci.* **34** (1977), 1155–1162.
- [25] J. Derber and A. Rosati, *A global oceanic data assimilation system.*, *J. Phys. Oceanogr.* **19** (1989), 1333–1347.
- [26] J. E. Geisler and D. E. Stevens, *On the vertical structure of damped steady circulation in the tropics.*, *Q.J.R. Meteorol. Soc.* **108** (1982), 87–93.
- [27] A. E. Gill, *Some simple solutions for heat induced tropical circulation*, *Q. J. R. Meteorol. Soc.* **106** (1980), 447–462.
- [28] M. H. Glantz, R. W. Katz, and N. Nicholls, *Scientific Basis and Societal Impact*, Cambridge University Press, Cambridge, England, 1990.
- [29] Goswami, B. N. and J. Shukla, *Predictability of a Coupled Ocean-Atmosphere Model*, *J. Climate* **4** (1991), 3–22.

- [30] N. E. Graham, J. Michaelson, and T. P. Barnett, *An investigation of the El Niño-Southern Oscillation cycle with statistical models. 1. Predictor field characteristics.*, J. Geophys. Res. **92** (1987a), 14251–14270.
- [31] ———, *An investigation of the El Niño-Southern Oscillation cycle with statistical models. 2. Model results.*, J. Geophys. Res. **92** (1987b), 14271–14290.
- [32] J. Hansen, I. Fung, A. Lacis, D. Rind, S. Lebedeff, R. Ruedy, and G. Russell, *Three-dimensional model*, J. Geophys. Res. **93** (1988), 9341–9364.
- [33] I. M. Held and M. J. Suarez, *A two-level primitive equation atmospheric model designed for climatic sensitivity experiments.*, J. Atmos. Sci. **35** (1978), 206–229.
- [34] A. C. Hirst, *Unstable and damped equatorial modes in simple coupled ocean-atmosphere models*, J. Atmos. Sci. **43** (1986), 606–630.
- [35] ———, *Slow instabilities in tropical ocean basin - global atmosphere models*, J. Atmos. Sci. **45** (1988), 830–852.
- [36] J. D. Horel and J. M. Wallace, *Planetary scale atmospheric phenomena associated with the Southern Oscillation.*, Mon. Wea. Rev. **109** (1981), 813–829.
- [37] M. Inoue and J. J. O’Brien, *A forecasting model for the onset of El Niño.*, Mon. Wea. Rev. **112** (1984), 2326–2337.
- [38] P. D. Jones, *The influence of enso on global temperatures.*, Climate Monitor **17** (1988), 80–89.
- [39] E. B. Kraus and J. S. Turner, *A one-dimensional model of the seasonal thermocline. II: The general theory and its consequences.*, Tellus **19** (1967), 98–106.
- [40] M. Latif, J. Biercamp, H. von Storch, and F. W. Zwiers, *A ten year climate simulation with a coupled ocean-atmosphere general circulation model.*, Max-Planck-Institut für Meteorologie, Report No. 21, no. 21, Bundesstrasse 55, D-2000 Hamburg 13, FRG, 1988.
- [41] Mojib Latif, Moritz Flügel, and Jin-Song Xu, *An investigation of short range climate predictability in the tropical Pacific*, J. Geophys. Res. (1991).
- [42] N. C. Lau, *Modeling the seasonal dependence of the atmospheric response to observed El Niños in 1962-76.*, Mon. Wea. Rev. **113** (1985), 1970–1996.
- [43] A. Leetmaa and M. Ji, *Operational hindcasting of the tropical pacific.*, Dyn. Atmos. Ocean. **13** (1989), 465–490.
- [44] J. P. McCreary, *Modeling equatorial ocean circulation.*, Ann. Rev. Fluid Mech. **17** (1985), 359–409.
- [45] G. A. Meehl, *Development of global coupled ocean-atmosphere general circulation models.*, Clim. Dyn. **5** (1990), 19–33.

- [46] ———, *Seasonal cycle forcing of El Niño-Southern Oscillation in a global coupled ocean-atmosphere gcm.*, J. Climate **3** (1990), 72–98.
- [47] M. Münnich, M. A. Cane, and S. E. Zebiak, *A study of self-excited oscillations of the tropical ocean atmosphere system. Part II: Nonlinear cases.*, J. Atmos. Sci. **48** (1991), 1238–1248.
- [48] J. D. Neelin, *Interannual oscillations in an ocean general circulation model coupled to a simple atmosphere model.*, Phil Trans Roy Soc Lond **329A** (1989), 189–205.
- [49] ———, *A hybrid coupled general circulation model for El Niño studies.*, J. Atmos. Sci. **47** (1990), 674–693.
- [50] ———, *The slow sea surface temperature mode and the fast-wave limit: Analytic theory for tropical interannual oscillations and experiments in a hybrid coupled model.*, J. Atmos. Sci. **48** (1991), 584–606.
- [51] J. D. Neelin, M. Latif, M. A. F. Allaart, M. A. Cane, U. Cubasch, W. L. Gates, P. R. Gent, M. Ghil, C. Gordon, N. C. Lau, G. A. Meehl, C. R. Mechoso, J. M. Oberhuber, S. G. H. Philander, P. S. Schopf, K. R. Sperber, A. Sterl, T. Tokioka, J. Tribbia, and S. E. Zebiak, *Tropical air-sea interaction in general circulation models.*, Climate Dyn., submitted, 1991.
- [52] R. C. Pacanowski and S. G. H. Philander, *Parameterization of vertical mixing in numerical models of tropical oceans*, J. Phys. Ocean. **11** (1981), 1443–1451.
- [53] S. G. H. Philander, *El Niño, La Niña, and the Southern Oscillation.*, Academic Press, San Diego, 1990.
- [54] S. G. H. Philander, W. J. Hurlin, and A. D. Siegel, *Simulation of the seasonal cycle of the tropical Pacific ocean.*, J. Phys. Oceanogr. **17** (1987), 1986–2002.
- [55] S. G. H. Philander, R. C. Pacanowski, N. C. Lau, and M. J. Nath, *A simulation of the Southern Oscillation with a global atmospheric GCM coupled to a high-resolution, tropical Pacific ocean GCM*, J. Climate **submitted** (1991).
- [56] S. G. H. Philander, T. Yamagata, and R. C. Pacanowski, *Unstable air-sea interactions in the tropics.*, J. Atmos. Sci. **41** (1984), 604–613.
- [57] W. H. Quinn, D. O. Dopf, K. S. Short, and R. T. W. Kuo-Yang, *Historical trends and statistics of the Southern Oscillation, El Niño, and Indonesian droughts.*, Fish. Bull. **76** (1978), 663–678.
- [58] W. H. Quinn, V. T. Neal, and E. A. De Mayolo, *El Niño occurrences over the past four and a half centuries*, J. of Geophys. Res. **92** (1987), 14,449–14461.
- [59] C. S. Ramage, *Sea surface temperature and local weather.*, Mon. Wea. Rev. **105** (1977), 540–544.

- [60] E. M. Rasmusson, *El Niño and variations in climate.*, Am. Sci. (1988), 168–177.
- [61] E. M. Rasmusson and T. H. Carpenter, *Variations in tropical sea surface temperature and surface wind fields associated with the Southern Oscillation/El Niño*, Mon. Wea. Rev. **110** (1982), 354–384.
- [62] R. W. Reynolds, K. Arpe, C. Gordon, S. P. Hayes, A. Leetmaa, and M. J. McPhaden, *A comparison of tropical Pacific surface wind analyses*, J. Climate **2** (1989), 105–111.
- [63] C. F. Ropelewski and M. S. Halpert, *Global and regional scale precipitation patterns associated with the El Niño/Southern Oscillation.*, Mon. Wea. Rev. **114** (1987), 2352–2362.
- [64] P. S. Schopf and Mark A. Cane, *On equatorial dynamics, mixed-layer physics and sea surface temperature*, J. Phys. Oceanogr. **13** (1983), 917–935.
- [65] P. S. Schopf and M. J. Suarez, *Vacillations in a coupled ocean-atmosphere model*, J. Atmos. Sci. **45** (1988), 549–566.
- [66] _____, *Ocean wave dynamics and the timescale of ENSO*, J. Phys. Oceanogr. **20** (1990), 629–645.
- [67] R. Seager, *Modeling tropical Pacific sea surface temperature: 1970-1987*, J. Phys. Oceanogr. **19** (1989), 419–434.
- [68] R. Seager, S. E. Zebiak, and Mark A. Cane, *A model of the tropical Pacific sea surface temperature climatology*, J. Geophys. Res. **93** (1988), 1265–1280.
- [69] J. Shukla and J. M. Wallace, *Numerical simulation of the atmospheric response to equatorial Pacific sea surface temperature anomalies.*, J. Atmos. Sci. **40** (1983), 1613–1630.
- [70] M. J. Suarez and P. S. Schopf, *A delayed action oscillator for ENSO*, J. Atmos. Sci. **45** (1988), 3283–7.
- [71] K.E. Trenberth, G.W. Branstator, and P.A. Arkin, *Origins of the 1988 North American drought*, Sci **242** (1988), 1640–1645.
- [72] B. C. Weare, *Interannual variation of net heating at the surface of the tropical Pacific Ocean*, J. Phys. Oceanogr. **13** (1983), 873–885.
- [73] _____, *A comparison of shallow water model results for three estimates of a composite El Niño forcing.*, J. Atmos. Sci. **43** (1986), 162–170.
- [74] B. C. Weare, T. Strub, and M. D. Samuel, *Annual mean surface heat fluxes in the tropical Pacific Ocean*, J. Phys. Oceanogr. **11** (1981), 705–717.
- [75] K. Wyrtki, *El Niño – The dynamic response of the equatorial Pacific Ocean to atmospheric forcing*, J. Phys. Oceanogr. **5** (1975), 572–84.

- [76] _____, *The response of sea surface topography to the 1976 El Niño*, J. Phys. Oceanogr. **9** (1979), 1223–1231.
- [77] Jin-Song Xu and Han von Storch, *Predicting the state of the Southern Oscillation using principal oscillation pattern analysis*, J. Climate **3** (1990), 1316–1329.
- [78] S. E. Zebiak, *A simple atmospheric model of relevance to El Niño.*, J. Atmos. Sci. **39** (1982), 2017–2027.
- [79] _____, *Atmospheric convergence feedback in a simple model for El Niño*, Mon. Wea. Rev. **114** (1986), 1263–1271.
- [80] S. E. Zebiak and M. A. Cane, *A model El Niño-Southern Oscillation*, Mon. Wea. Rev. **115** (1987), 2262–2278.
- [81] _____, *Natural climate variability in a coupled model.*, Workshop on Greenhouse-Gas-Induced Climate Change: A Critical Appraisal of Simulations and Observations (Michael E. Schlesinger, ed.), Oregon State University, 1989.
- [82] Stephen E. Zebiak, *Diagnostic Studies of Pacific Surface Winds*, J. Climate **3** (1990), 1016–1031.
- [83] Y Zhao, M. Cane, and S. E. Zebiak, *Comparison of El Niño as recorded in the Quelccaya ice-cap and a coupled dynamical model*, in preparation (1991).

Figure Captions

Fig.1a: Time series of NINO3 from 1024-year simulations with the coupled model of Zebiak and Cane (1987). NINO3 denotes SST anomalies averaged over the region 5°N to 5°S , 90°W to 150°W . It is a widely used index of ENSO events, since warm anomalies in the NINO3 area are characteristic of El Niño (viz Figs. 2-4). (a) A run with Standard parameter settings, characteristic of the present climate (see Sec 3). (b) A run with the background conditions of Greenhouse Scenario I, in which it is simplistically assumed that tropical ocean warms uniformly by 1°C (see Sec. 3).

Fig.2: Coupled model SST anomalies for March and December during a coupled model El Niño event (note that the contour interval for March is 0.25°C and that for December is 0.5°). (From Cane and Zebiak, 1985).

Fig.3: First four EOF's of the ZC model SST anomalies, calculated from monthly values of the 1024-year simulation shown in Fig 1a.

Fig.4: First four EOF's of observed SST anomalies, calculated from monthly values between the years 1970 and 1987, inclusive (CAC analysis).

Fig.5: Time-longitude sections for 16 years of the ZC coupled model integration showing the forcing for the gravest mode oceanic Kelvin wave, a measure of zonal wind anomalies along the equator. Positive (westerly) anomalies are indicated with solid lines, and negative (easterly) anomalies are indicated with dashed lines. Large westerly anomalies ($.15\text{dynes}/\text{cm}^2$) are stippled. (From Cane and Zebiak 1985.)

Fig.6: Time-longitude history of the Schopf and Suarez (1988) coupled model anomalies averaged between 2S and 2N . (a) SST. Contour interval 0.5C . (b) Ocean surface height (a good proxy for thermocline displacement or upper ocean heat content). Contour interval = 1 cm . (c) Lower-level zonal wind. Contour interval = 0.2 ms^{-1} . Negative anomalies are hachured. (From Schopf and Suarez, 1988).

Fig.7: Time-longitude behavior of the Schopf and Suarez coupled model, illustrating the equatorial wave dynamics of the oscillation mechanism. (a) (η_R) , the sea level displacements of Rossby waves averaged between 5 and 7 degrees of latitude, from 80°W (on left) to 120°E (on right). (b) (η_K) , the sea level displacements of equatorial Kelvin waves from 120°E to 120°W . (c) U , zonal surface wind on the equator from 180°W to 125°W . (d) (η_R) from 160°W (onleft) to 120°E . (e) (η_K) from 120°E to 80°W . In (a) - (c) positive anomalies are hachured. In (d) and (e) negative anomalies are hachured. (From Schopf and Suarez, 1988.) The leftmost panel (a) shows the westward propagation of "warm" (positive sea level anomaly) Rossby waves, originating near the center of the basin. At the western boundary they reflect as warm Kelvin waves which cross to the east (b). The warming at the east results in positive (westerly) wind anomalies (c). These in turn force "cold" Rossby waves (d), initiating the cold phase of the cycle.

Fig.8: Time series of NINO3 from a 1024 year simulation of the ZC coupled model using Greenhouse Scenario II (see text). Compare with Figs 1a,b.

Fig.9: Sea surface temperature anomalies in January 1987 as observed (top) and as forecast from January 1986 (bottom). The observed field is actually the product produced by the Climate Analysis Center (CAC)/NOAA. The forecasting procedure is described in Cane et al (1986).

Fig.10: Model forecasts (dashed line) and observed (solid line) NINO3 SST anomalies (C) from 1970 to 1989. The forecasts are at the various lead times indicated; a zero-month lead forecast is actually the initial condition generated by the ocean model forced by observed winds. (From Cane, 1990.)

Fig.11: A summary of the forecasting skill of the ZC model based procedure of Cane et al (1986). Shown is the correlation coefficient of forecast and observed NINO3 SST anomalies at lead times for 0 to 24 months. The Correlation of a Persistence forecast with observed values is also shown. A value of 0.5 marks a forecast with the same error variance as a climatological forecast.

Fig.12: (A) Forecasts at 3-month lead times by the Graham et al (1987) statistical M1A versus observations. The symbol “nf” indicates no forecast and occurs when the prediction model does not show statistically significant skill. The arrow labeled “ocean model” shows the time (May) when the Inoue and O’Brien (1984) model M2 forecasted an El Niño to occur during the next 3-month period centered on July. (B) Three-month lead forecasts by model ZC dynamical versus observations. (C) Nine-month lead forecasts by the statistical model versus observations. (D) As in (C), but from the dynamical model.

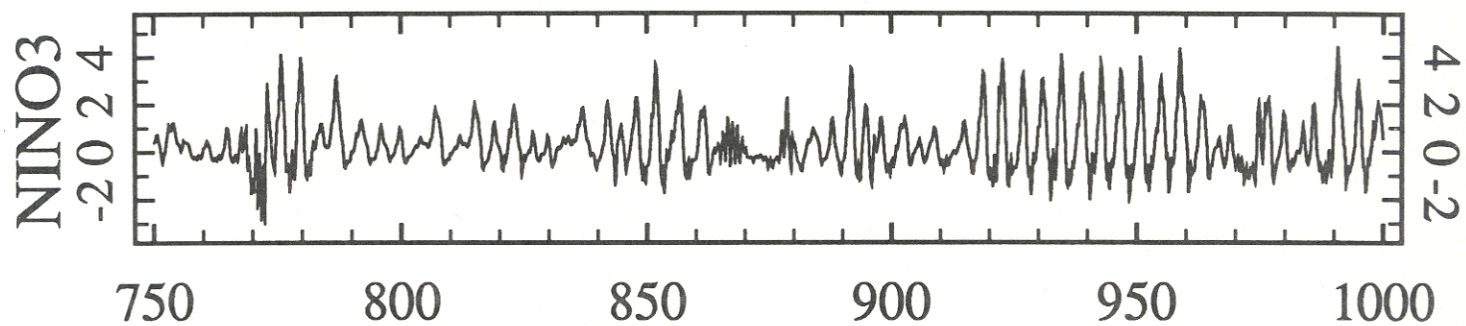
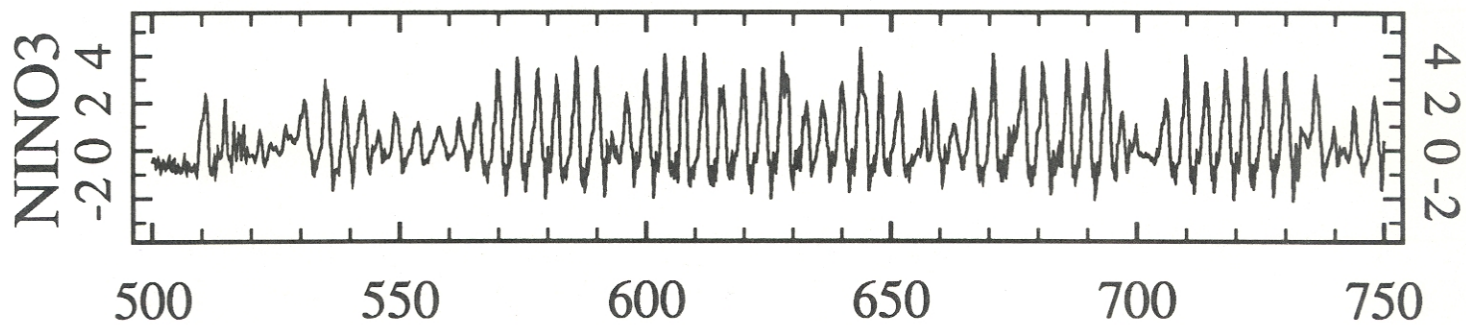
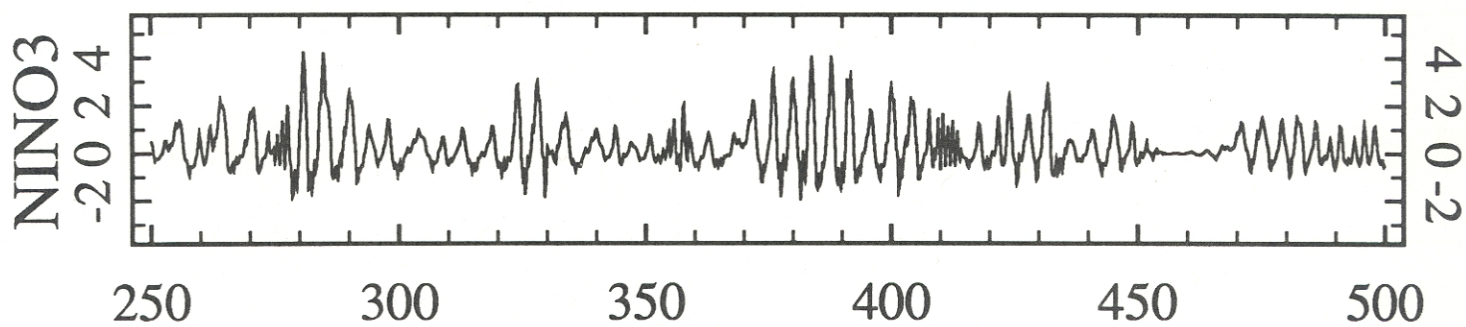
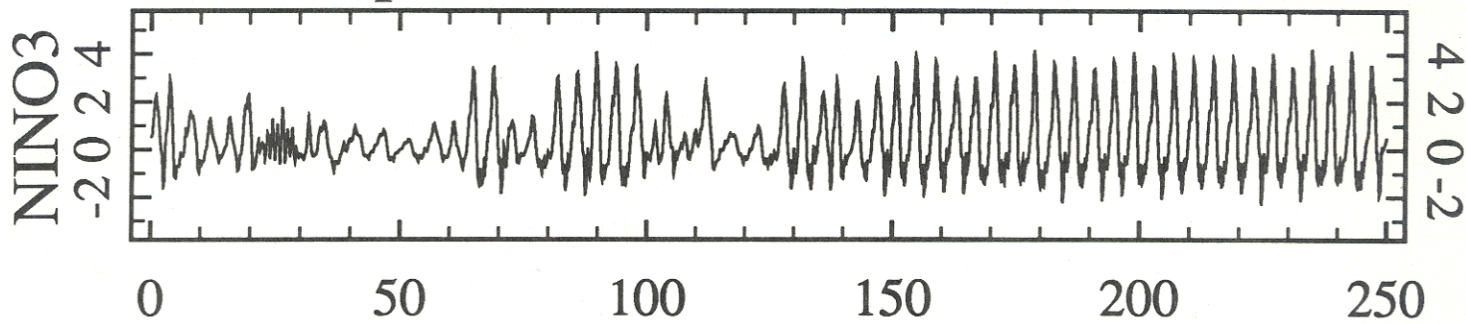
Fig.13: The hindcast skill of the Xu and von Storch (1990) forecast scheme. Shown is the correlation coefficient of the observed and predicted amplitudes of the ENSO POP as a function of the lag (see text). Correlations ≥ 0.5 mark forecasts which are considered skillful (they have less error variance than the climatological forecast). The POP forecast loses (hindcast) skill after 8 months, whereas a conventional univariate ARMA model and persistence pass the 0.5 line after about 5 months. (From Xu and von Storch, 1990.)

Fig.14: Pacific SST along the equator over 9 years of simulation (without seasonal cycle) with the hybrid model of Neelin (1990). Contour interval 0.5°C .

Fig.15: Time-longitude plot of seasonal mean differences from the long-term seasonal means for years 21-30 in the coupled model of Meehl (1990), 50°E to 80°W , averaged from 10°N to 10°S . Vertical line near center is the date line; horizontal lines demarcate the seasonal boundary between northern spring (MAM) and northern summer (JJA): (a) SST. Stippling greater than $+0.5^{\circ}\text{C}$, hatching less than -0.5°C . (b) SLP. Stippling less than -0.5 mb, hatching greater than $+0.5$ mb. (c) u-component wind stress. Stippling greater than $+0.1 \text{ dyn cm}^{-2}$ ($+0.01 \text{ N m}^{-2}$), hatching less than -0.1 dyn cm^{-2} (-0.01 N m^{-2}). (d) Precipitation. Stippling greater than $+0.5 \text{ mm day}^{-1}$, hatching less than -0.5 mm day^{-1} . (From Meehl, 1990.)

Fig.16: Pacific SST along the equator over 28 years of simulation (without seasonal cycle) by the coupled model of Philander et al (1991). Smoothing by a 13-month running mean has been applied. Contour interval 0.5°C , shaded over 28°C . (From Neelin et al 1991.)

Coupled Model - Standard Parameters



Time in Years

Coupled Model - Greenhouse Scenario I

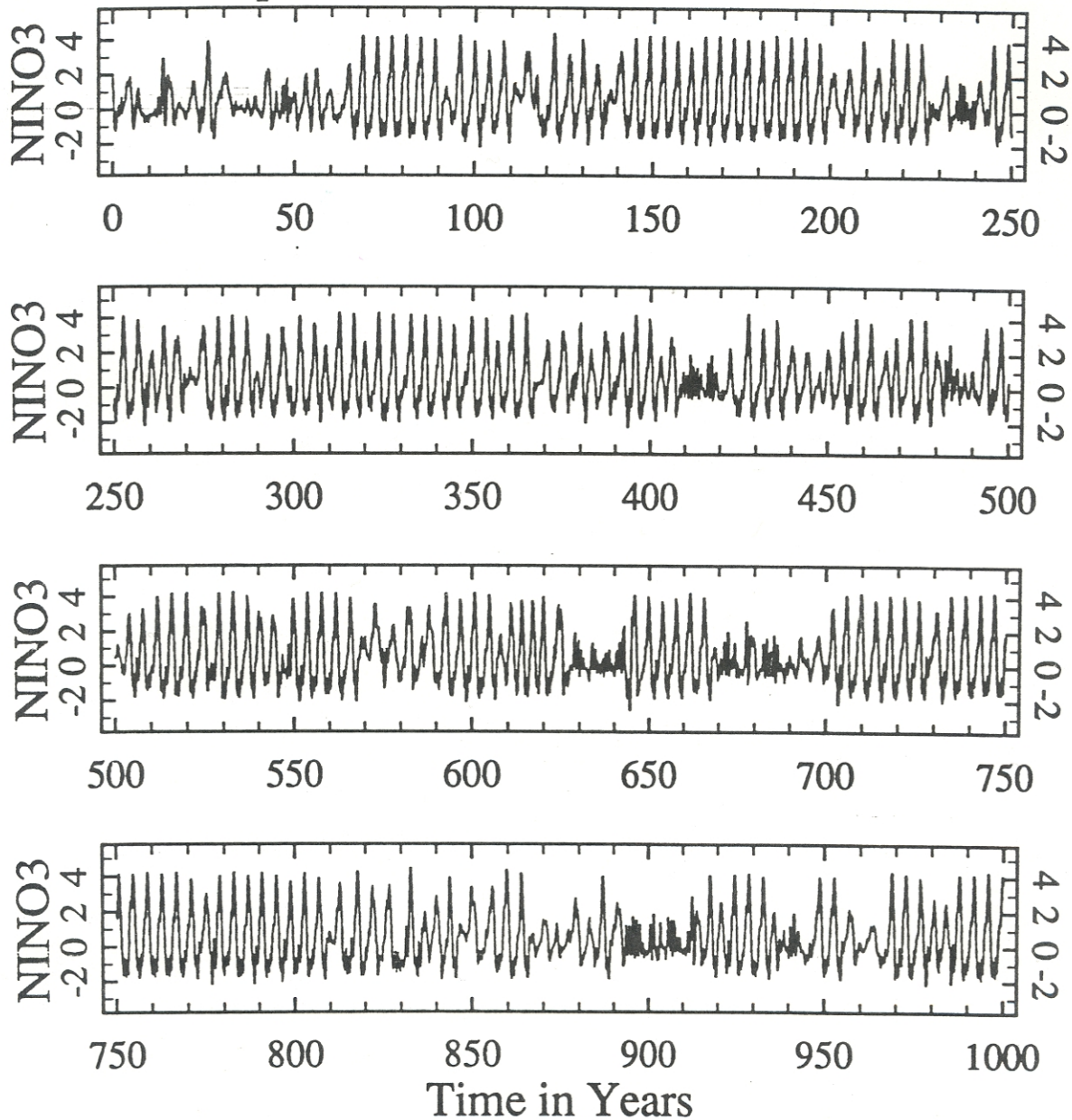


FIG. 1b Time series of NINO3 from a 1000 year simulation of the coupled model using Greenhouse Scenario I (see text).

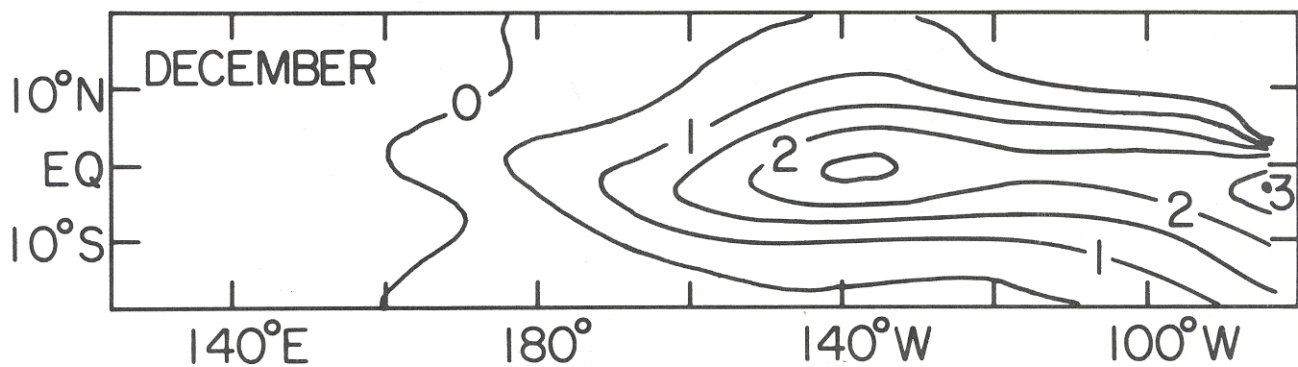
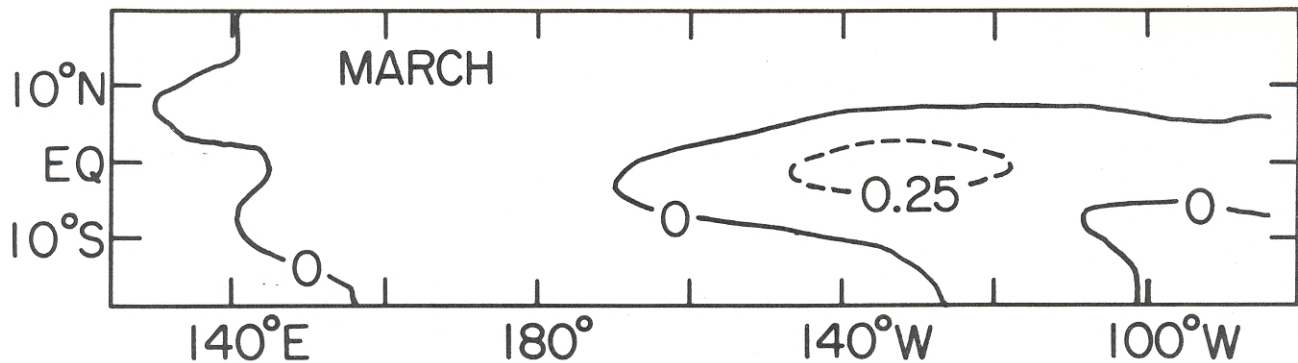


Fig. 2 Coupled model SST anomalies for March and December during the model El Niño event in year 31 (note that the contour interval for March is 0.25 C and that for December is 0.5). (From Cane & Zebiak, 1985)

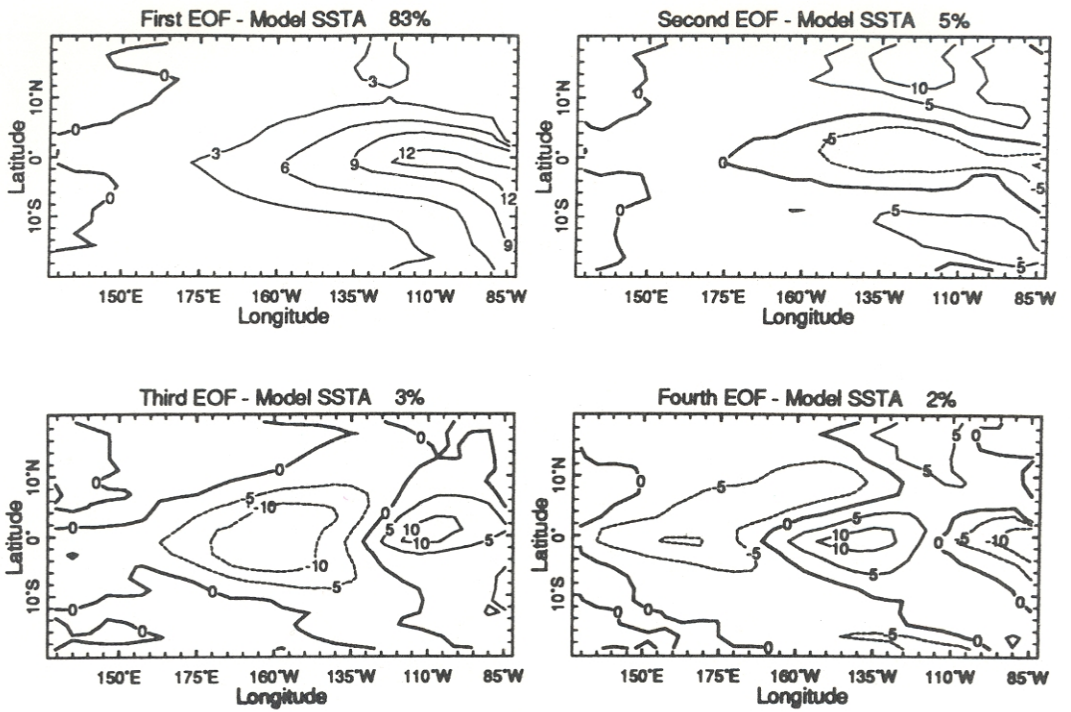


FIG. 3 First four EOF's of the model SST anomalies, calculated from monthly values of the 1024-year simulation.

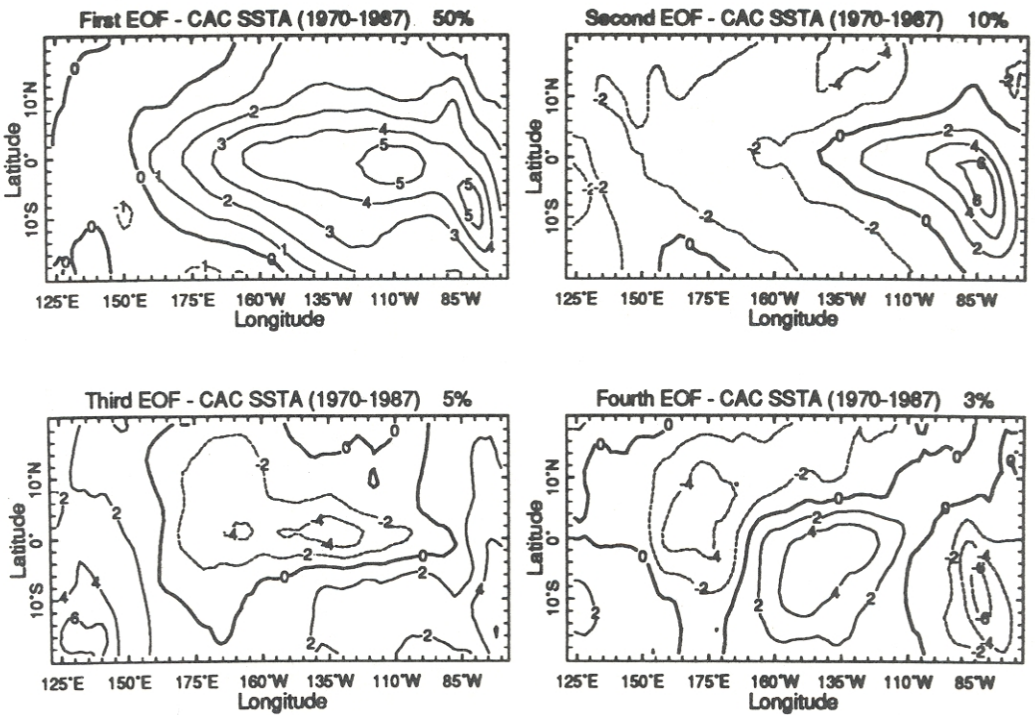


FIG. 4 First four EOF's of observed SSTA anomalies, calculated from monthly values between the years 1970 and 1987, inclusive (CAC analysis).

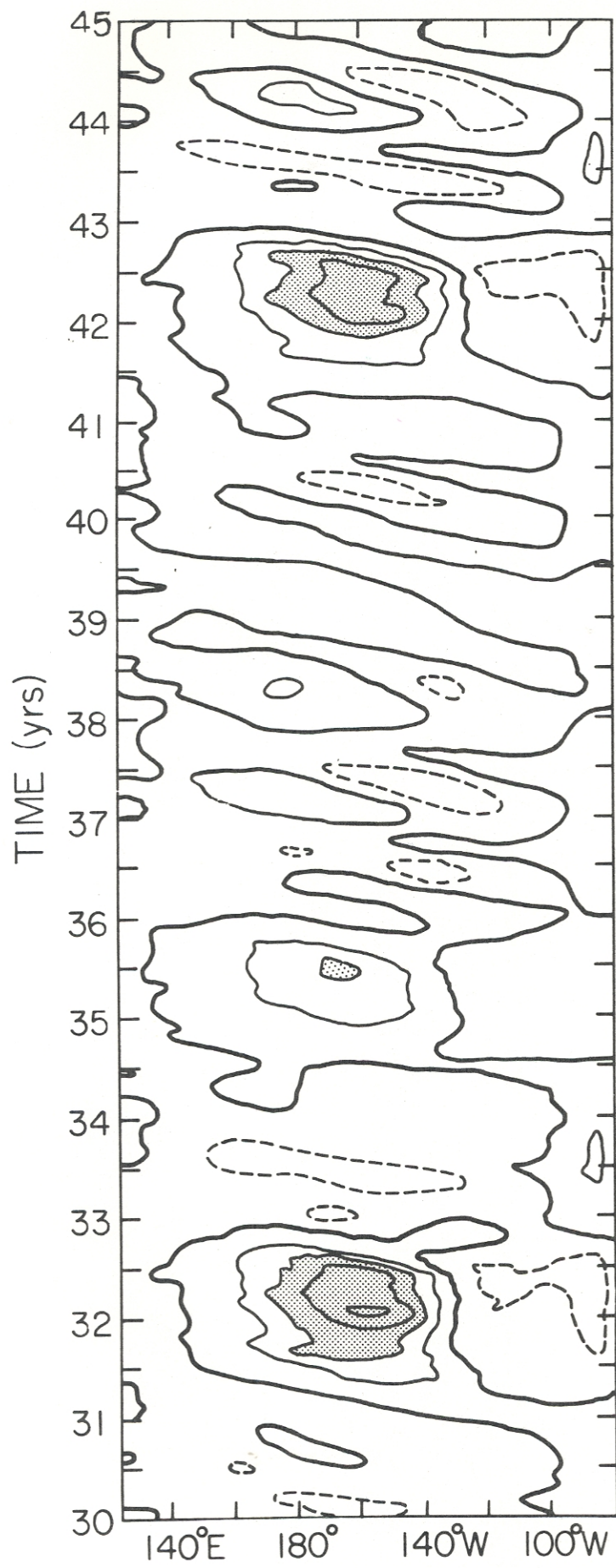


Fig. 5 Time-longitude sections for years 30-45 of the coupled model integration showing the forcing for the gravest mode oceanic Kelvin wave, a measure of zonal wind anomalies along the equator. Positive (westerly) anomalies are indicated with solid lines, and negative (easterly) anomalies are indicated with dashed lines. Large westerly anomalies ($.15 \text{ dynes/cm}^2$) are stippled.

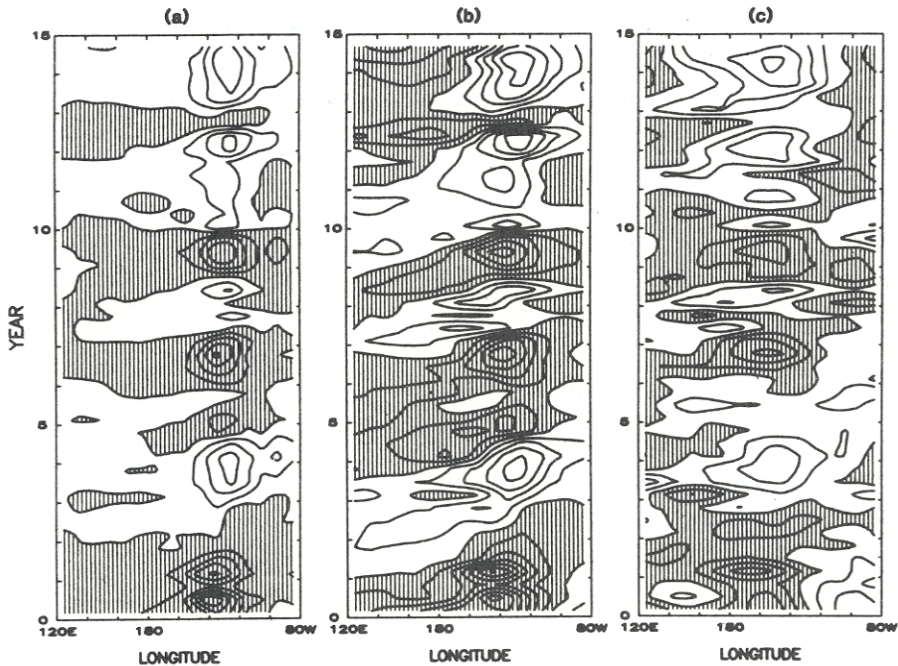


FIG. 6 Time-longitude history of model anomalies averaged between 2°S and 2°N for the first 15 years of the run: (a) SST. Contour interval = 0.5°C. (b) Ocean surface height (η_K). Contour interval = 1 cm. (c) lower-level zonal wind. Contour interval = 0.2 m s⁻¹. Negative anomalies are hachured.

(from Schoft & Suarez, 1988)

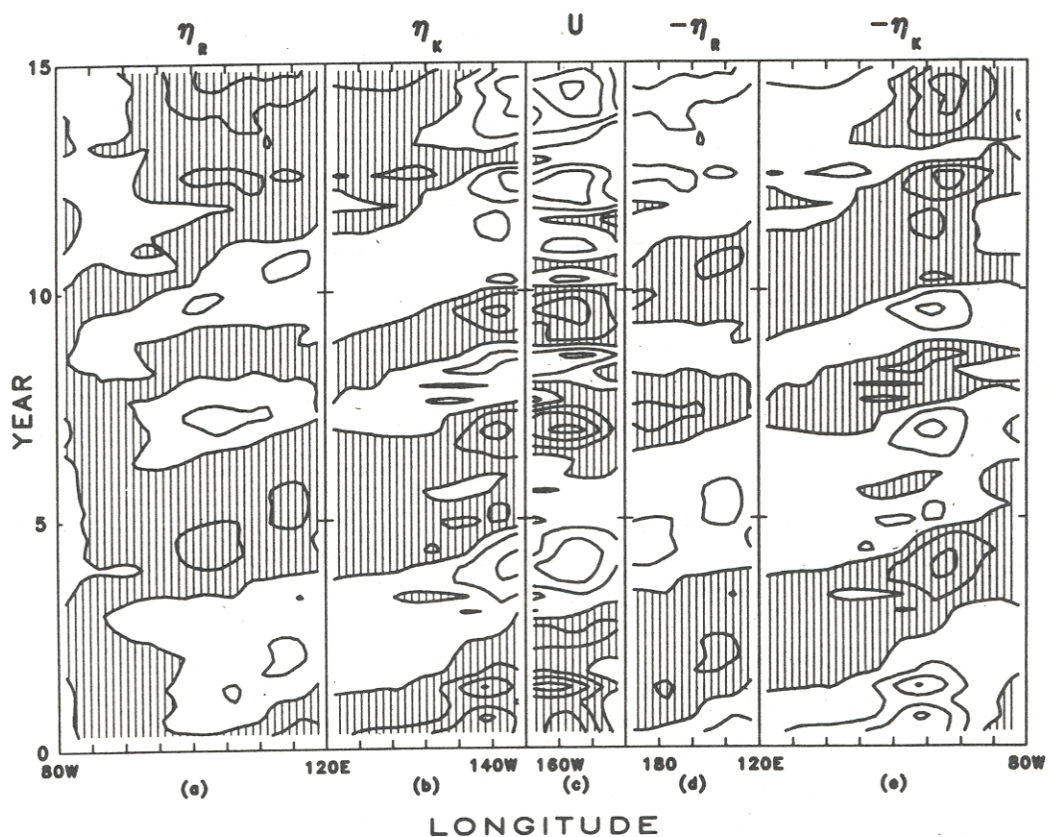


FIG. 7 Time-longitude behavior of the coupled model oscillator. (a) η_R from 80°W (on left) to 120°E (on right). (b) η_K from 120°E to 120°W. (c) Zonal surface wind on equator from 180°W to 125°W. (d) η_R from 160°W (on left) to 120°E. (e) η_K from 120°E to 80°W. In (a)-(c) Positive anomalies are hatched. In (d) and (e) negative anomalies are hatched.

Coupled Model - Greenhouse Scenario II

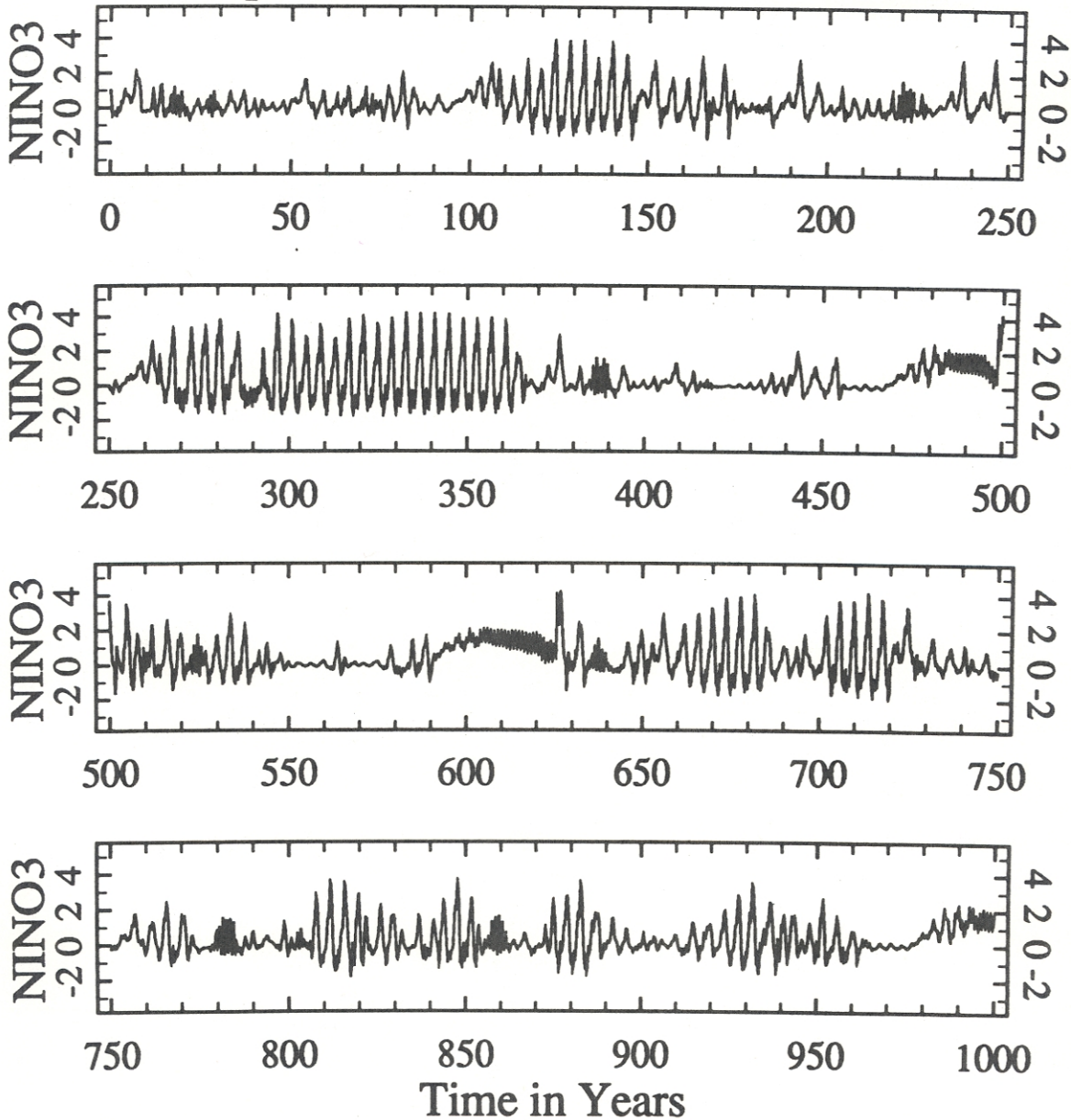


FIG. 8 Time series of NINO3 from a 1000 year simulation of the coupled model using Greenhouse Scenario II (see text).

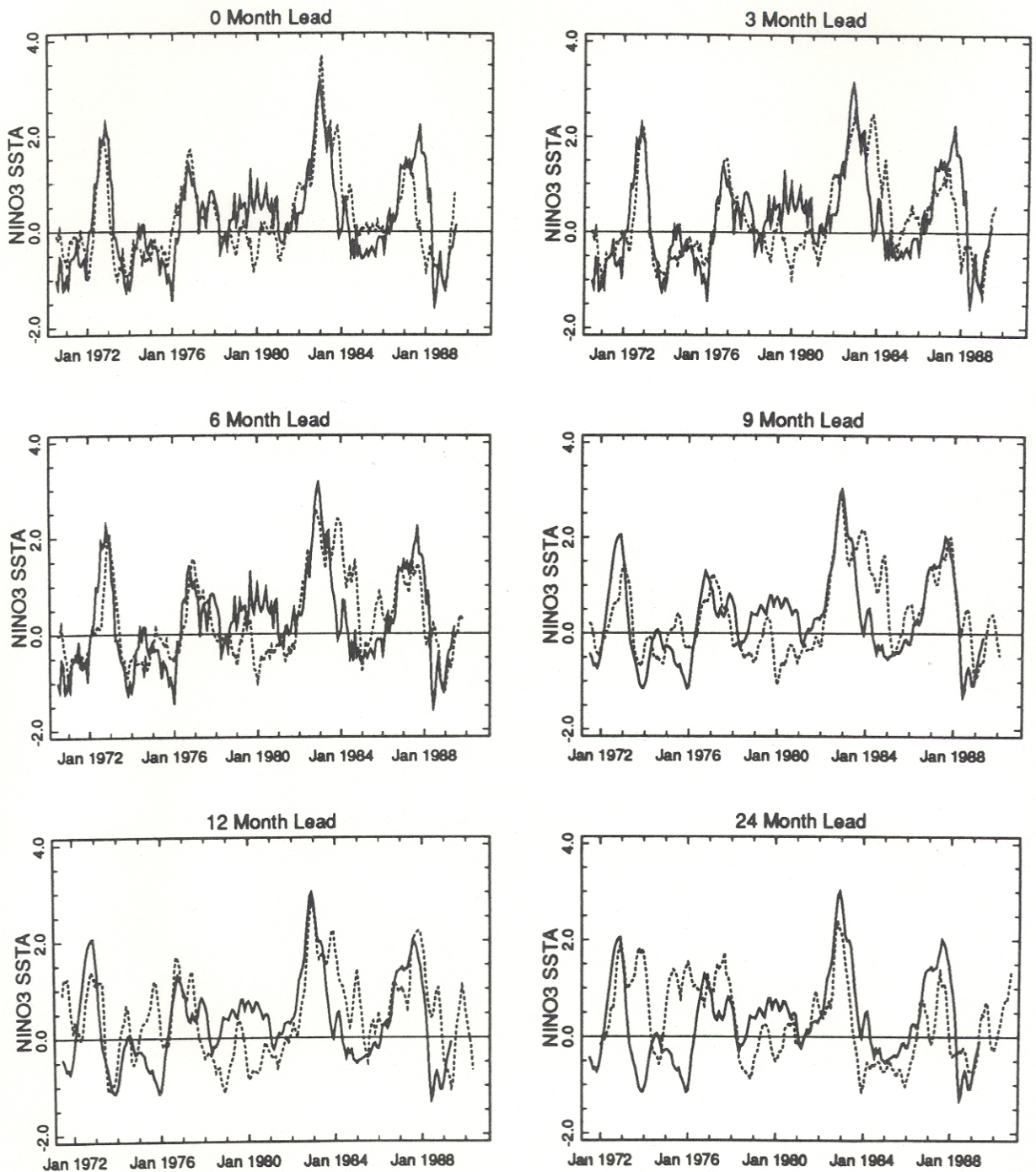


Fig.10: Model forecasts (dashed line) and observed (solid line) NINO3 SST anomalies (C) from 1970 to 1989. The forecasts are at the various lead times indicated; a zero-month lead forecast is actually the initial condition generated by the ocean model forced by observed winds. (From Cane, 1990.)

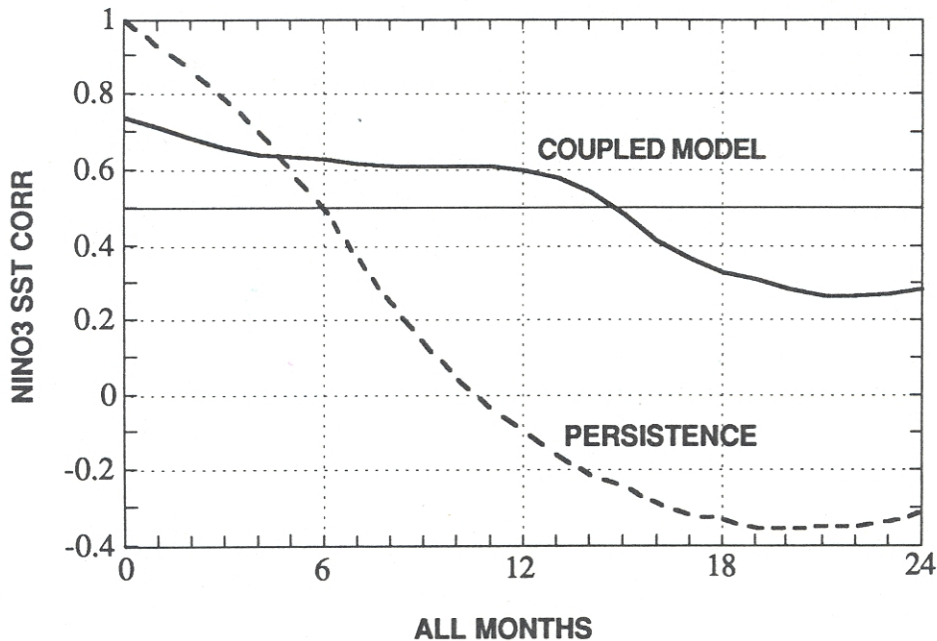
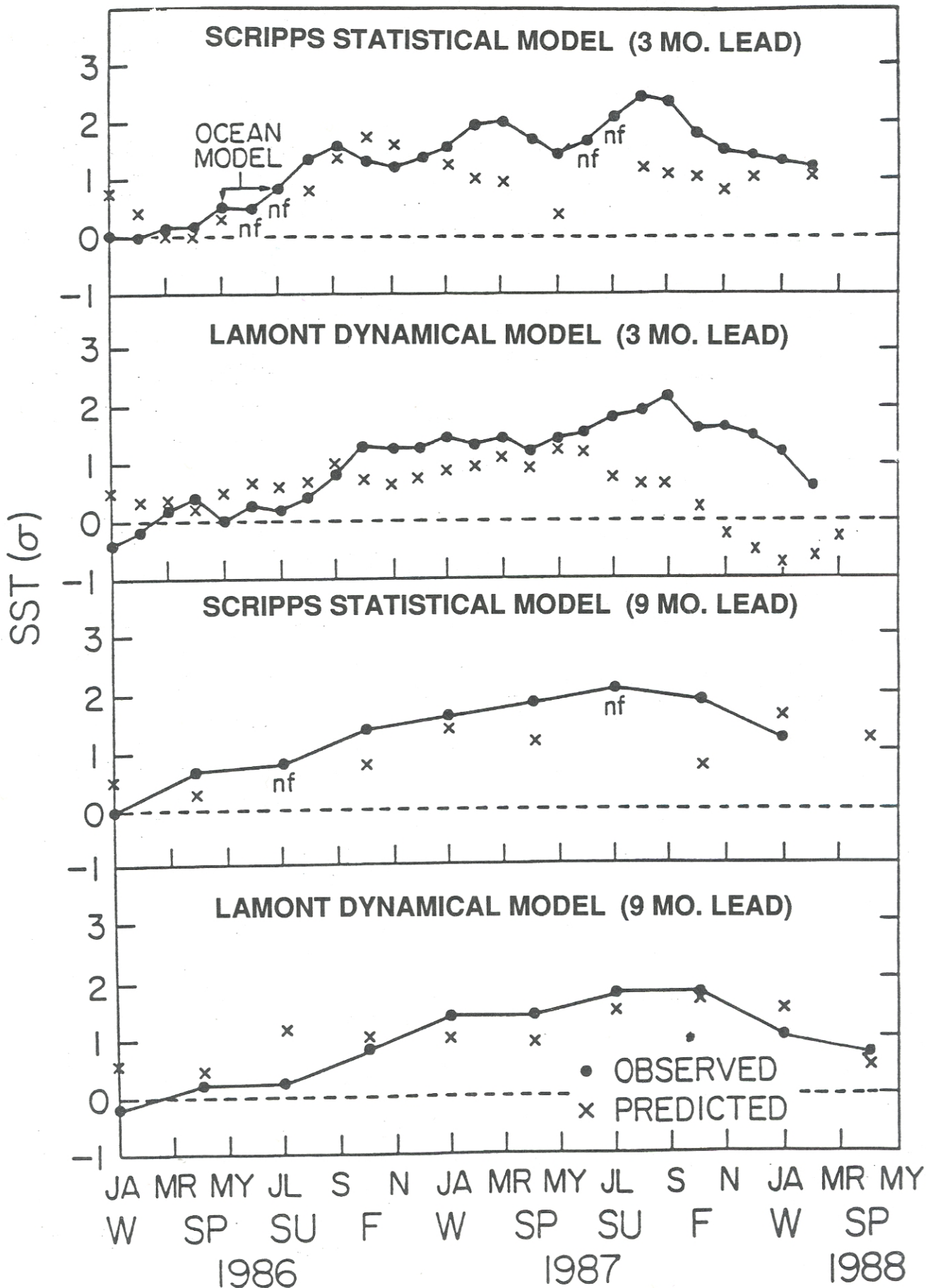


Fig.11: A summary of the forecasting skill of the ZC model based procedure of Cane et al (1986). Shown is the correlation coefficient of forecast and observed NINO3 SST anomalies at lead times for 0 to 24 months. The Correlation of a Persistence forecast with observed values is also shown. A value of 0.5 marks a forecast with the same error variance as a climatological forecast.

SST FORECAST vs. OBSERVATION

(from Barnett et al.,
Science, 1988)



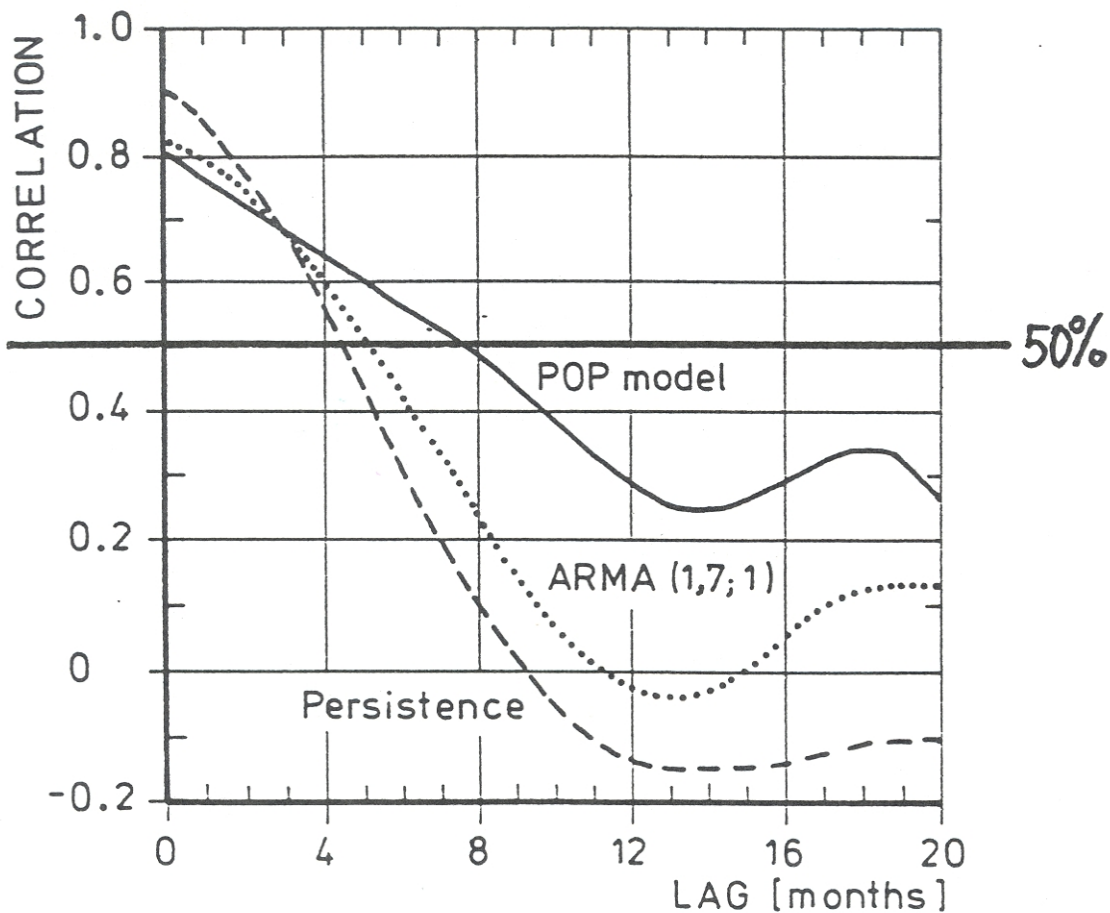
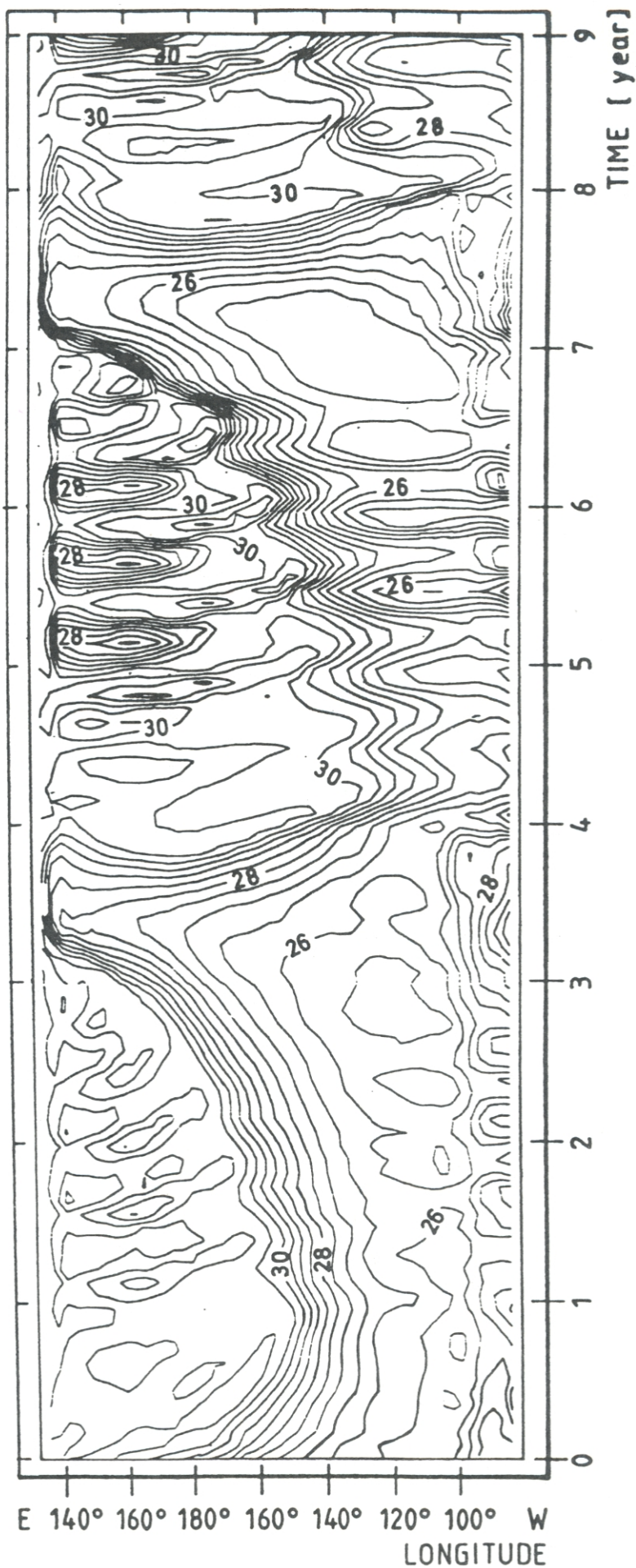
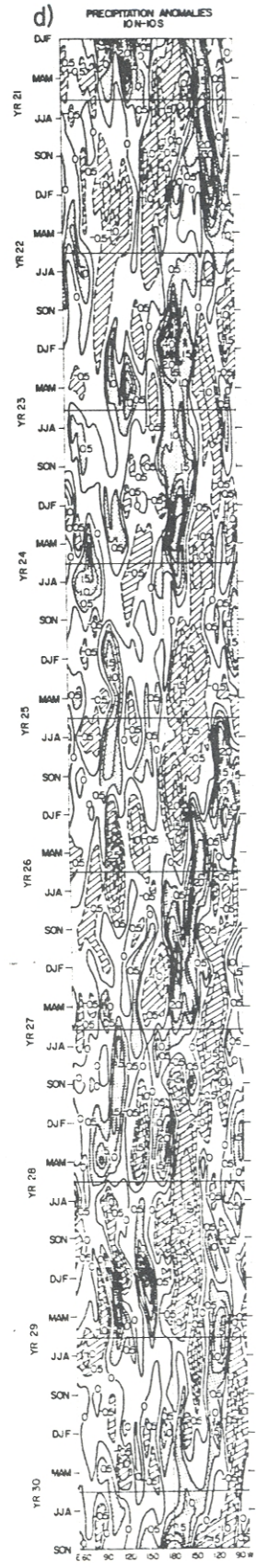
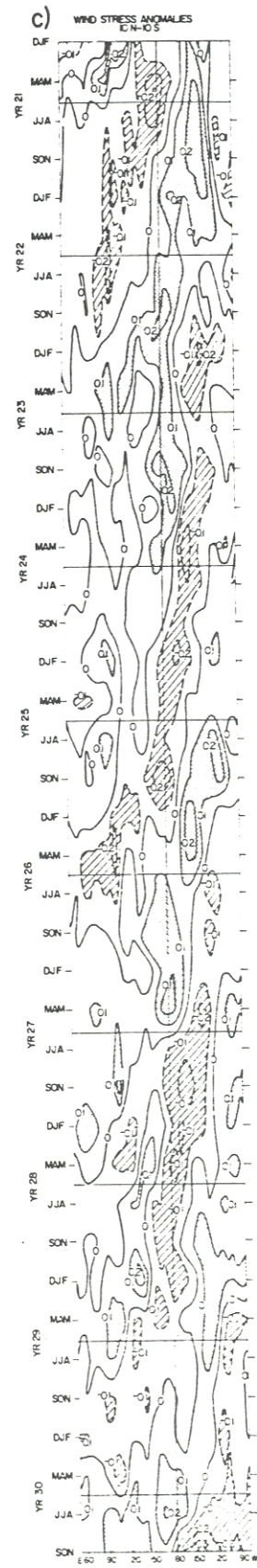
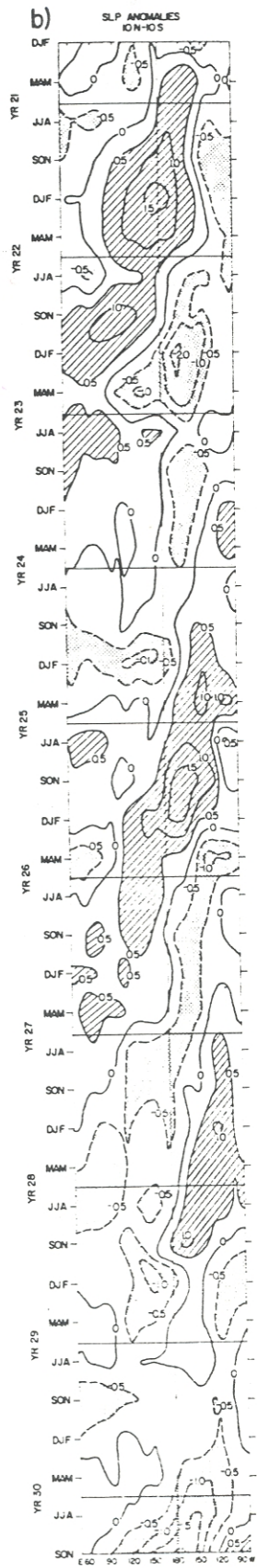
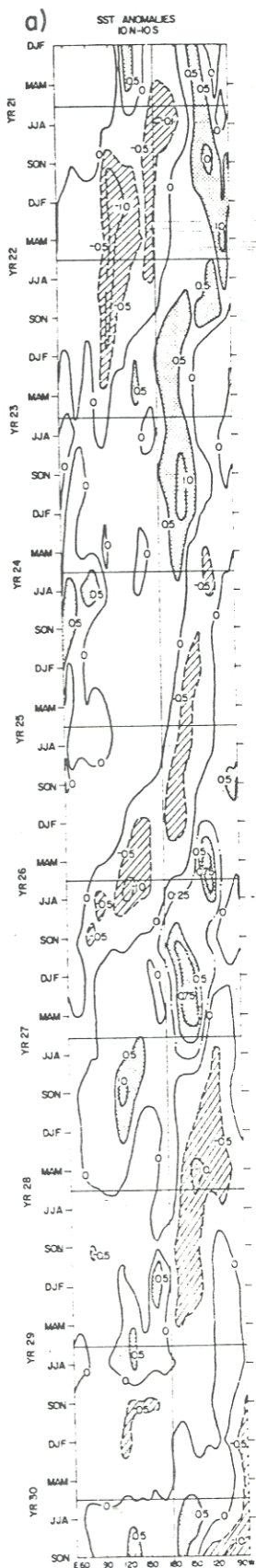
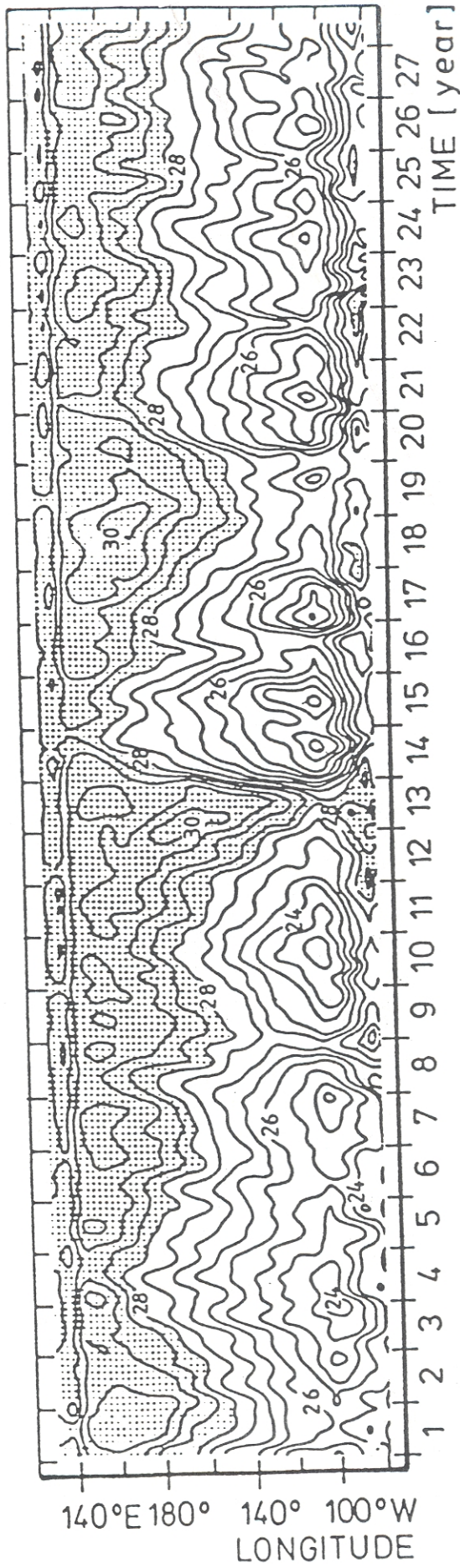


Fig.13: The hindcast skill of the Xu and von Storch (1990) forecast scheme. Shown is the correlation coefficient of the observed and predicted amplitudes of the ENSO POP as a function of the lag (see text). Correlations > 0.5 mark forecasts which are considered skillful (they have less error variance than the climatological forecast). The POP forecast loses (hindcast) skill after 8 months, whereas a conventional univariate ARMA model and persistence pass the 0.5 line after about 5 months. (From Xu and von Storch, 1990.)







060MOL

140°E 180° 140° 100°W
LONGITUDE

TIME [year]